

12-1-1993

DETECTION OF HARMONIC LOADS ON A POWER SYSTEM UNDER PRACTICAL CONDITIONS OF NON-SINUSOIDAL VOLTAGES AND VARIABLE FREQUENCY

Naveen Jaluria

Purdue University School of Electrical Engineering

Follow this and additional works at: <http://docs.lib.purdue.edu/ecetr>

Jaluria, Naveen, "DETECTION OF HARMONIC LOADS ON A POWER SYSTEM UNDER PRACTICAL CONDITIONS OF NON-SINUSOIDAL VOLTAGES AND VARIABLE FREQUENCY" (1993). *ECE Technical Reports*. Paper 259.
<http://docs.lib.purdue.edu/ecetr/259>

This document has been made available through Purdue e-Pubs, a service of the Purdue University Libraries. Please contact epubs@purdue.edu for additional information.

DETECTION OF HARMONIC LOADS
ON A POWER SYSTEM UNDER
PRACTICAL CONDITIONS OF
NON-SINUSOIDAL VOLTAGES
AND VARIABLE FREQUENCY

NAVEEN JALURIA

TR-EE 93-52
DECEMBER 1993



SCHOOL OF ELECTRICAL ENGINEERING
PURDUE UNIVERSITY
WEST LAFAYETTE, INDIANA 47907-1285

**DETECTION OF HARMONIC LOADS ON A POWER SYSTEM UNDER
PRACTICAL CONDITIONS OF NON-SINUSOIDAL VOLTAGES
AND VARIABLE FREQUENCY**

Naveen Jalaria

Purdue Electric Power Center
School of Electrical Engineering
Purdue University
1285 Electrical Engineering Building
West Lafayette, IN 47907-1285

December 1993

ACKNOWLEDGMENTS

First of all I will like to express my gratitude to the Purdue Electric Power Center for supporting me during my research at Purdue, and for giving me an opportunity to look at some of the problems affecting the utility industry. Especially I will like to thank Prof. Ong for his time, effort and continued support all along the way. Were it not for his ideas at crucial points, the research could have drifted in an unwanted direction. I will also like to thank Prof. O. Wasynczuk and Prof. J. Krogmeier for serving as members of my advisory committee.

TABLE OF CONTENTS

	Page
LIST OF TABLES	v
LIST OF FIGURES	vi
ABSTRACT	viii
CHAPTER 1 INTRODUCTION	1
1.1. Causes of Harmonics	1
1.2. Practical Problems Encountered Because of Harmonics.....	2
1.3. Need for Power Quality Standards.....	3
1.4. Motivation.....	4
1.5. Outline of the Thesis	4
CHAPTER 2 POWER FLOW IN A CIRCUIT WITH A NONLINEAR LOAD	6
2.1. Power Flow in a Linear Electrical Circuit	6
2.2. Relation between Voltage and Current Harmonics.....	7
2.3. Analysis of Instantaneous Power.....	11
2.3.1. Interpretation of the Analysis of Instantaneous Power.....	15
2.4. Analysis of Power Flow in a Circuit with a Nonlinearity	16
2.4.1. Calculation of the Instantaneous Power	17
2.4.2. Interpretation of the Direction of Average Power Flow in a Nonlinear Circuit	20
2.5. Average Power Analysis in Terms of Phasors.....	21
2.6. Definition of Harmonic Loads.....	24
2.7. Definition of Distortion	25
CHAPTER 3 EXPERIMENTAL SET UP AND DETAILS	27
3.1. Details of the Experimental Set up and Components.....	27
3.2. Analysis of the Acquired Data	28
3.3. Experiment 1	
A Computer Monitor Load	29
3.3.1. Determination of Direction of Average Power Flow.....	31
3.3.2. Interpretation of the Results for Experiment 1.....	33

	Page
3.4. Applicability of the Method to Other Nonlinear Harmonic Loads	33
3.5. Experiment2	
A Fluorescent Lamp Load	33
3.5.1. Determination of the Direction of the Active Power.....	35
3.6. Details of Experimentation and Analysis	36
3.6.1. Inadequacy of the Cross-Spectrum of the Instantaneous Power.....	39
 CHAPTER 4 FAST FOURIER TRANSFORM AND ITS PROPERTIES	48
4.1. Properties of Fast Fourier Transform.....	48
4.2. Errors Involved in FFT.....	51
4.2.1. Spectral Leakage Errors in FFT.....	51
4.2.2. Picket Fence Effect	53
 CHAPTER 5 AUTOMATION OF THE HARMONIC LOAD DETECTION PROCESS USING NEURAL NETWORKS	57
5.1. Need for Neural Net approach.....	57
5.2. Introduction to the Neural Network Application.....	58
5.3. Back Propagation Algorithm.....	59
5.4. Use of the Neural Net on the Computer Monitor data.....	61
5.4.1. Structure of the Neural Net Algorithm	61
5.4.2. Testing of the Load Data Using the trained Neural Net	63
 CHAPTER 6 RECOMMENDED APPLICATION OF THE DETECTION TECHNIQUE.....	68
6.1. Conclusion	68
6.2. Detection Technique Configuration	69
6.3. Suggestions for Future Research.....	70
 BIBLIOGRAPHY.....	72

LIST OF TABLES

Table	Page
1. FFT Analysis of the Voltage and Current Drawn by the Computer Monitor.....	30
2. FFT Analysis of the Voltage and Current Drawn by a 40W Fluorescent Lamp.....	34
3. A sample of the Input FFT Data and the Desired Output as given to Neural Net for Training.....	64
4. Average Harmonic Powers for Computer Monitor given by Neural Net.....	65

LIST OF FIGURES

Figure	Page
1. A diode being fed from an ideal sinusoid sources.....	7
2. A diode being fed from a practical source.....	9
3. A complex ac voltage source feeding a given load.....	11
4. Fundamental voltage and current phasors for a diode load.....	21
5. Voltage and current phasors at the second harmonic frequency for the diode load.....	21
6. Voltage and current phasors at the third harmonic frequency for the diode load.....	22
7. Domains of the current phasor for capacitive, inductive and harmonic loads.....	25
8. Experimental set up for the voltage and current data acquisition for a load.....	40
9. Block diagram for the analysis of the experimentally acquired data.....	41
10. Waveforms of the voltage applied to and current drawn by the computer monitor.....	42
11. Harmonic components of the voltage waveform fed to the computer monitor.....	43
12. Harmonic components of the current drawn by the computer monitor.....	44
13. Waveforms of the voltage applied to and the current drawn by the fluorescent lamp.....	45
14. Harmonic components of the voltage fed to the fluorescent lamp.....	46

Figure	Page
15. Harmonic components of the current drawn by the fluorescent lamp.....	47
16. Position of two adjacent side lobes for minimum spectral leakage effect.....	56
17. A single neuron which takes N inputs and forms a weighted output.....	59
18. Structure of the net used to identify harmonic peaks in FFT Data.....	61
19. Voltage harmonic peaks detected by neural net.....	67
20. Measurements taken iteratively at different customer points.....	71

ABSTRACT

The purpose of this work is to develop an on-line measurement technique, which could be used iteratively to detect the presence of harmonic loads on the power system. This has to be achieved in an environment of non-sinusoidal voltage **waveforms** and variable frequency as is the case in practice. This is achieved by looking at the relative phase relationship between the voltage and current at each **harmonic** frequency. From this information, the average **harmonic** power flowing in the load circuit can be found out. **If the** load is injecting average power back to the source at harmonic frequencies, then it can be called a harmonic source. The method has been applied successfully to a variety of load **data** which have been collected experimentally.

CHAPTER 1. INTRODUCTION

Before the introduction of power electronics in ac power networks the presence of higher frequencies (above the fundamental frequency of 60 Hz), called **harmonics** in general terms, in the power system was mainly from space harmonics of the generator windings, from core saturation of transformers and generators, and to a lesser extent from loads like the mercury arc rectifiers. In general harmonics came on the ac power systems because of nonlinearities in generation and distribution rather than because of the presence of nonlinear loads on the system. The effect of these harmonics on the system was not significant and of little or no practical interest. With the advent of power electronics and the proliferation of such equipment since **1960s**, the presence of harmonics **in** power systems has become pronounced and the voltage waveform, at a given point on the power system has deviated from its sinusoidal nature.

1.1. Causes of Harmonics

The main causes of distortions in the present day power systems **are** nonlinear semiconductor loads. Power electronic equipment is being used heavily in various static power converters. This usage varies typically from a household appliance: taking in a few watts of power through to large pulse width modulated variable speed control drive system and rectifiers used in the manufacturing industry. Power convertors are **also** used in electrochemical power supplies, uninterruptible power supplies and switched mode computer power supplies. Induction arc furnaces, **arc** discharge devices, **railway** transit systems and fluorescent lighting also add to the list of nonlinear loads present on the power

system. The presence of High Voltage DC (HVDC) transmission systems further adds to the creation of harmonics on the ac side of the convertor. Some of these **equipment** distort the voltage directly, others inject currents of distorted shape which in turn produces **non-sinusoidal** voltage drop across series elements in the network causing **distortion** of the bus voltages. The resultant effect of all these harmonic loads on the system **has been** detrimental to power quality.

The current and voltage **harmonics** are mostly interrelated, because: the series voltage drop caused in the circuit due to current harmonics introduces voltage harmonics on the system. This interrelation of the current and voltage harmonics will be explained more precisely further along.

1.2. Practical Problems Encountered Because of Harmonics

The presence of harmonics on the system can cause a lot of practical problems to various users. The presence of harmonic currents on the system interferes with the **normal** operation of communication circuits, appearing as unwanted noise on the communication channel. One of the major problem encountered by customers and utilities; alike is the cause of compensation capacitor bank failure due to harmonic resonance [13]. Capacitor banks which offer a low impedance path to higher harmonics may overload and fail due to increased dielectric loss. This resonance may also occur with reactive components of the network, creating sustained overvoltages. It has been observed that when two or three capacitor banks are in service there is a significant fifth harmonic current present [13]. Depending on the phase angle relation between the fundamental and fifth harmonic the peak voltage on the capacitor could exceed that normally permitted, thus causing the capacitor to fail on **occasion**.

The presence of harmonic current causes increased eddy current and hysteresis losses in the iron cores of transformers, motors, fluorescent light ballast, etc. This

additional heating losses results in lower operating efficiencies and possible failure of the equipment due to higher temperature. Harmonic also have the capacity to cause subharmonic mechanical oscillations of the turbine shaft of a generator. They can also cause maloperation of relays, sensitive semiconductor equipment and the accuracy of induction watt-hour meters.

1.3. Need for Power Quality Standards

From the above description of some of the problems that **harmonics** can cause, it is evident that a limit has to be set on the flow of harmonics on the power system.

Determining the maximum allowable limits of a particular harmonic on the system will depend on the practice. Harmonic standards have been introduced all over the world.

IEEE standard 519 [16] serves as a guideline for designing systems with linear and nonlinear loads. It also defines the quality of power to be supplied by the utility to the consumer at the point of common coupling. At the same time this **standard** tries to define the allowable harmonic current injection from individual customers back to the utility, in order to maintain acceptable voltage distortion levels on the system.

In enforcing the standards, it will be necessary to determine who, the utility or the consumer is responsible for some or all of the distortion. As such it will be useful to be able to determine within reasonable accuracy the loads responsible for the generation of harmonics. Once we locate the loads responsible, corrective action can be taken to prevent the flow of harmonics into the system. This corrective action can be in the form of series or parallel line shunt filters, to filter out certain trouble some harmonics. Various methods have been devised by researchers in the past to measure the harmonic flows at a particular point, to determine the exact source of a particular harmonic [10].

1.4. Motivation

The objective of this thesis is to come up with a technique to be able to pinpoint any load which is a source of harmonics. Under the perfect condition of a **sinusoidal** voltage waveform it is very easy to identify any harmonic loads on the system. This can be done by detecting the presence of current harmonics from the load in the absence of any voltage harmonics. But under practical conditions of non-sinusoidal voltage **wave** shape it is not that easy. First of all the bus voltage waveform by itself is not purely sinusoidal. In such a case the presence of current **harmonics** is not a clear cut indication of the **nature** of the load. This situation calls for a need to have a closer look at the process of harmonic generation and propagation. The very purpose of this work here is to be able to detect any harmonic load on the power system even when the supply voltage is not purely **sinusoidal** and its frequency drifts around the fundamental.

1.5. Outline of the Thesis

Chapter **2** begins with an examination of the relationship between voltage and current harmonics. The phenomenon of average power flow of a linear **and** non-linear circuit, in the presence of harmonic voltages has been observed. Particular attention is given to the direction of average power at various harmonic frequencies. Section **2.4** deals with analysis of average power flow in a circuit with a known nonlinearity. The phenomenon of negative average power flow at certain frequencies is **observed**. This phenomenon is exploited in a method which has been used for detecting such nonlinearities.

The usefulness of the proposed method for detecting harmonic (nonlinear) loads has been substantiated by experimentation in Chapter 3. The **experimental** set up and related details are described in this chapter. A brief explanation of the **signal** analysis technique, Fast Fourier Transform, used for analysing the stored data has also been provided here. Experiments have been performed on a variety of **common** harmonic loads

like computer monitor, fluorescent lamp, ac adjustable speed pulse width modulated (PWM) drive and an arc welder. The results have been noted down and shown to be conforming to the definition of harmonic loads.

Chapter 4 describes some mathematical properties of the Fast Fourier Transform, along with the identification of possible sources of inaccuracies, and means of reducing certain errors in the FFT analysis are mentioned.

Chapter 5 deals with the neural net implementation of this detection technique. The neural net has been trained to detect the harmonic frequency peaks from the FFT analysis, for the voltage or current waveform data. The neural net has been tested on the computer monitor load data taken from Chapter 3. The average powers flowing at different frequencies to this load have been determined and once again the load has proven to be a harmonic load.

Chapter 6, suggests future research that can be done in solving this detection problem. We have also discussed a possible iterative technique for the use of this method in practice to locate harmonic loads on the network.

CHAPTER 2. POWER FLOW IN A CIRCUIT WITH A NONLINEAR LOAD

2.1. Power Flow in a Linear Electrical Circuit

From basic circuit theory we know that applying a sinusoidal voltage across a linear load results in a sinusoidal current flow. If the linear load is purely resistive then the current waveform is in phase with the voltage waveform. If the linear load is a purely inductive circuit then the current will lag the voltage by 90°, but if it is a purely capacitive circuit the current will lead the voltage by 90°. In the case of a resistive load the direction of power flow is from the source to the load. All the average power flow occurs at the fundamental frequency only. But for the purely capacitive or inductive loads there is no net transfer of energy. Power flow alternates from the source to load for one half cycle and from load to the source for the other half cycle.

In all the above mentioned cases we are assuming the absence of any voltage or current harmonics. Only the fundamental component (60Hz) of the current and voltage is assumed present in the circuit. The introduction of a harmonic load instead of a pure resistor or a pure inductor or capacitor, affects the average power flows of harmonic components in a rather interesting way. To get to that point, let us begin with the basics of how the harmonics are generated in a given controlled environment, and how they propagate and how they effect the supply voltage waveform in that particular circuit, and eventually how all this affects the average power flow in this particular circuit.

2.2. Relation between Voltage and Current Harmonics

The presence of current harmonics causes a non-sinusoidal voltage drop in the circuit impedance. This circuit impedance can be either the load impedance, source impedance or both. The output voltage waveform of the source would be altered if the source has some source impedance. If there were no circuit impedance, and the load was a harmonic load like a diode, then ideally speaking in that case the current waveform will be only half wave rectified. It will be zero over the non-conducting half cycle for the diode. The **fourier** analysis of such a current wave shape will show the presence of harmonic components in it. That is, it will contain the fundamental **60Hz**, and along with that it will contain a number of other sinusoidal components at frequencies which are exact multiples of the fundamental (that is **120 Hz, 180 Hz, 240 Hz, 300 Hz ...**). The proper addition of all these components, up to the highest possible harmonic will result in the distorted current wave shape we actually started with.

Lets us assume the controlled environment as mentioned above where the effect of the load current on the source voltage distortion is negligible. In other words the source impedance is negligible such that current harmonics do not have any kind of effect on the sinusoidal nature of the voltage waveform. This case has been shown in Fig. 1.

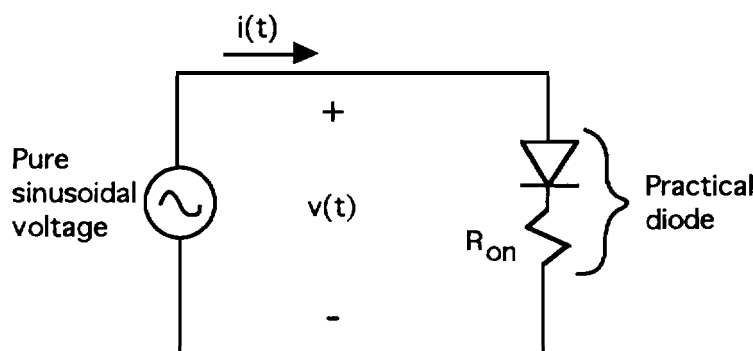


Figure 1 A diode being fed from an ideal sinusoid source

Such a case is hard to realize in real life systems. There is always source impedance and there is always load impedance, along with any nonlinearity in circuit if any. For the sake of explanation of the phenomenon let us look at **some of** the properties of this idealized circuit once again. The **current** waveform here is half wave rectified and it is periodic all along. The Fourier series of this current waveform shows the presence of the fundamental and harmonic frequencies. The voltage waveform never gets distorted. The real power flowing in the circuit will be positive that is from the **source** to the load. This positive power flow signifies the flow of energy from the source to the load over a full cycle. Let us look at these power flows in a little detail.

$$v(t) = V_{m1} \sin(\omega_0 t) \quad \dots (2.1)$$

is the instantaneous applied voltage to the diode circuit. V_{m1} is the peak value of the fundamental frequency.

Now the conduction current of the diode is limited by the conduction resistance R_{on} of the diode. The Fourier series of the current waveform is given as is (2.2).

$$i(t) = I_{m1} \sin(\omega_0 t) + I_{m2} \sin(2\omega_0 t) + I_{m3} \sin(3\omega_0 t) + I_{m4} \sin(4\omega_0 t) + I_{m5} \sin(5\omega_0 t) + I_{m6} \sin(6\omega_0 t) + \dots \quad \dots (2.2)$$

$i(t)$ is the instantaneous current flowing in this circuit. $I_{m1}, I_{m2}, I_{m3}, \dots$ are the peak values of the fundamental, 2nd, 3rd, harmonic currents respectively.

The Fourier components of the current as evident in the **expansion** of $i(t)$, show the presence of the harmonic components of the **currents**. The fundamental frequency ω_0 of the current corresponds to the fundamental frequency of the voltage. **Harmonic** current components are introduced because of the nonlinearity of the load (**i.e. diode** in this present case).

The instantaneous power flowing to the diode is

$$p_{inst} = v(t) * i(t) \quad \dots (2.3)$$

Since $v(t)$ is a pure sinusoid the average power has only a contribution from the fundamental current component, that is the average (real) power

$$P_{avg} = (V_{m1} * I_{m1}) / 2 \quad \dots (2.4)$$

The expression for the instantaneous power p_{inst} contains this constant term P_{avg} , which is the average (real) power flowing in the circuit. Also p_{inst} contains some sine and cosine terms for the frequencies which are exact multiples of the fundamental frequency. These **sinusoidal** terms represent the reactive power flowing in the circuit at their respective frequencies. The net power transfer by these sinusoidal terms over a full cycle is zero. Thus, they only represent a pulsating power flow in the circuit. The total average power flowing in the circuit, as given by equation (2.4), is coming from the fundamental voltage and current components only.

Now let us **look** at an actual circuit which has a source resistance R_s , a circuit resistance R_c and the conduction resistance of the diode ' R_{on} ' as shown in the figure 2.

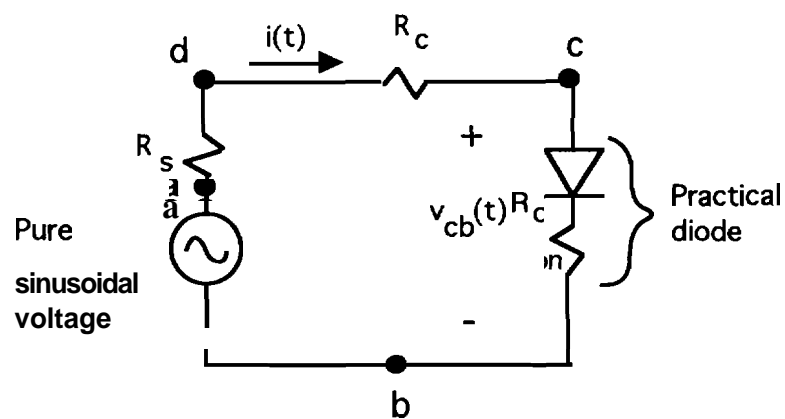


Figure 2 A diode being fed from a practical source

Due to the nonlinearity of the diode once again the current is not purely sinusoidal. As a result the voltage drop in the total resistance $R = (R_c + R_s + R_{on})$ is not purely sinusoidal. This harmonic current causes harmonic voltage drops across R , which in turn introduces harmonics in the supply voltage at the load terminals 'cd'. To be precise the voltage across the points 'c' and 'd' will not be sinusoidal any more, even though a pure voltage source is being used. The voltage across the points 'a' and 'b' will remain unchanged as the source is a pure sinusoidal source. This fact is explained mathematically below.

Consider the case when the pure voltage supplied by the source is

$$v_{ab}(t) = V_{m1} \sin(\omega_0 t) \quad \dots (2.5)$$

The current $i(t)$ flowing in the circuit is the same as that given above in **equation** (1.2).

Under these circumstances the voltage appearing across the diode is not sinusoidal. that is

$$\begin{aligned} v_{cb} &= v_{ab}(t) - i(t) * R \\ &= V_{m1} \sin(\omega_0 t) - R * \{ I_{m1} \sin(\omega_0 t) + I_{m2} \sin(2\omega_0 t) + I_{m3} \sin(3\omega_0 t) + I_{m4} \\ &\quad \sin(4\omega_0 t) + I_{m5} \sin(5\omega_0 t) + I_{m6} \sin(6\omega_0 t) \dots \dots \dots \} \quad \dots (2.6) \end{aligned}$$

Thus we see that the presence of harmonics in current $i(t)$ causes the appearance of harmonics in the voltage $v_{cd}(t)$ across the load terminals. Thus the voltage that is being applied to the diode is no longer sinusoidal. Hence it is clear from the above explanation that the current harmonics do cause voltage harmonics to occur in any nonlinear circuit. And the same explanation is true the other way around. The voltage harmonics cause current harmonics to flow in the circuit, even though the load may or may not be a harmonic load.

The above example is a very simple illustration of how the voltage and current harmonics can be interrelated. This interrelation is equally applicable to all kinds of load.

2.3. Analysis of Instantaneous Power

Lets us look at the Figure 3, where a non-sinusoidal voltage source is feeding a linear resistive load.

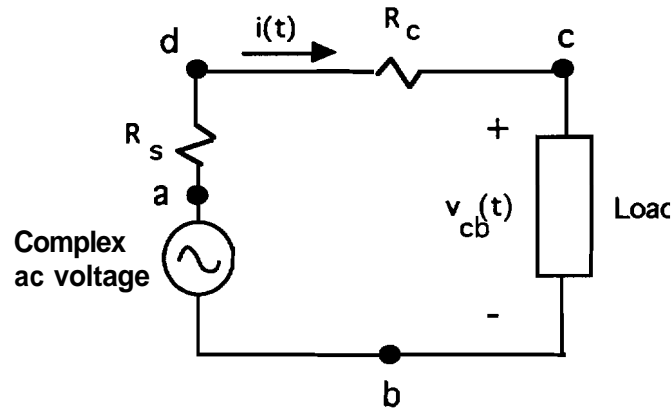


Figure 3. A complex ac voltage source feeding a given load

For analysis purposes let us say that this voltage waveform is a flat topped wave, such that the top and bottom of the sinusoid is clipped at $\sqrt{3}/2$ of its ~~peak~~ magnitude on both the half cycles. The only assumption here is that this voltage waveform is periodic in nature. The flat topped sinusoid is not uncommon nowadays in power outlets. Now lets us look at the power flow in a situation where a pure resistor is being fed from such a source. If V_m is the peak value of the unclipped voltage then the Fourier components of the applied waveform are given as

$$v_{cb}(t) = V_m \{ 0.845 \sin(\omega_0 t) + 0.05305 \cos(2\omega_0 t) + 0.23312 \cos(3\omega_0 t + 260.2^\circ) \\ + 0.011368 \cos(4\omega_0 t) + 0.0239096 \cos(5\omega_0 t + 73.9^\circ) + 0.00909 \cos(6\omega_0 t + 180^\circ) \\ + 0.06735 \cos(7\omega_0 t - 87.17^\circ) + 0.002526 \cos(8\omega_0 t) + 0.108806 \cos(9\omega_0 t) \}$$

$$\begin{aligned}
& + 267.910) + 0.001607 \cos(10\omega_0 t) + 0.0455 \cos(11\omega_0 t - 88.33^\circ) + 0.00222 \\
& \cos(12\omega_0 t + 180^\circ) + 0.03914 \cos(13\omega_0 t - 88.63^\circ) + \dots \dots \dots \} \\
& \dots \quad (2.7)
\end{aligned}$$

Similarly the current flowing in this circuit will be given as

$$\begin{aligned}
i(t) &= v_{cb}(t)/R. \\
&= (V_m/R) * \{ 0.845 \sin(\omega_0 t) + 0.05305 \cos(2\omega_0 t) + 0.23312 \cos(3\omega_0 t + 260.2^\circ) \\
&+ 0.011368 \cos(4\omega_0 t) + 0.0239096 \cos(5\omega_0 t + 73.9^\circ) + 0.00909 \cos(6\omega_0 t + \\
&180^\circ) + 0.06735 \cos(7\omega_0 t - 87.17^\circ) + 0.002526 \cos(8\omega_0 t) + 0.108806 \cos(9\omega_0 t + \\
&267.91^\circ) + 0.001607 \cos(10\omega_0 t) + 0.0455 \cos(11\omega_0 t - 88.33^\circ) + 0.00222 \\
&\cos(12\omega_0 t + 180^\circ) + 0.03914 \cos(13\omega_0 t - 88.63^\circ) + \dots \dots \dots \} \\
&= I_m * \{ 0.845 \sin(\omega_0 t) + 0.05305 \cos(2\omega_0 t) + 0.23312 \cos(3\omega_0 t + 260.2^\circ) + \\
&0.011368 \cos(4\omega_0 t) + 0.0239096 \cos(5\omega_0 t + 73.9^\circ) + 0.00909 \cos(6\omega_0 t + 180^\circ) \\
&+ 0.06735 \cos(7\omega_0 t - 87.17^\circ) + 0.002526 \cos(8\omega_0 t) + 0.108806 \cos(9\omega_0 t + \\
&267.91^\circ) + 0.001607 \cos(10\omega_0 t) + 0.0455 \cos(11\omega_0 t - 88.33^\circ) + 0.00222 \\
&\cos(12\omega_0 t + 180^\circ) + 0.03914 \cos(13\omega_0 t - 88.63^\circ) + \dots \dots \dots \} \\
&\dots \quad (2.8)
\end{aligned}$$

where I_m represents the peak value of the unclipped current **sinusoid**. Note that as expected with a linear load, its current and voltage have exactly the same harmonic components. The instantaneous power flowing to this circuit given by the product of the instantaneous voltage and current is

$$\begin{aligned}
p_{inst} &= (V_m * I_m) * \{ 0.39598 + 0.0557 \cos(\omega_0 t + 267.35) + 0.5588 \cos(2\omega_0 t + \\
&176.2) + 0.03356 \cos(3\omega_0 t - 88.5) + 0.1666 \cos(4\omega_0 t + 14.54) + 0.008155 \\
&\cos(5\omega_0 t + 104.8) + 0.0797 \cos(6\omega_0 t - 11.37) + 0.01894 \cos(7\omega_0 t + 268.8) +
\end{aligned}$$

$$0.16608 \cos(8\omega_0 t + 178.51) + 0.00856 \cos(9\omega_0 t - 84.76) + 0.14573 \cos(10\omega_0 t + 3.69) + 0.000291 \cos(11\omega_0 t + 264.56) + 0.029113 \cos(12\omega_0 t + 169.18) + 0.001736 \cos(13\omega_0 t - 87.73) + \dots \quad \dots \quad (2.9)$$

The instantaneous power has a constant term of **0.39598** and various other sinusoidal terms at harmonic frequencies. The constant term represents the average (real) power flowing in the circuit, while the various sinusoidal terms represent the reactive power flowing in this circuit at different **harmonic** frequencies. The total average power is the sum of the average power resulting from the fundamental voltage and **current** components and the average powers resulting from the various current and voltage harmonic components . All these components of the average power add up to give the total average power being consumed by the resistive load.

Each sinusoidal term in the instantaneous power has a **contribution** from the direct product of each of sinusoidal terms in the voltage to every other term in the current waveforms. These sinusoidal terms in the instantaneous power represent the reactive power flow, and this power is pulsating in nature. Its average over one cycle is zero. This reactive power does no useful work in the circuit. Since these reactive harmonic power components are a sum total of the components emerging from the multiplication of various combinations of the voltage and current harmonic components, it is not easy to trace the origin of harmonic reactive power to any of the individual voltage or current harmonic components. It is a sum total of contributions to that frequency from **various** other frequencies.

On the other hand the constant term found above can be traced directly to the contributions from the individual frequencies. It is clearly seen that the average power at any frequency can be directly found from the product of the current and voltage

components at that frequency. Let us look at how this total average power comes out from the individual frequency components.

The total average power flow in the circuit is $(0.39598 \cdot V_m \cdot I_m)$

Now the fundamental components in the voltage and **current** waveforms are given as:

$$v_1(t) = V_{m1} \cos(\omega_0 t) = 0.845 V_m \cos(\omega_0 t - 90^\circ)$$

$$i_1(t) = I_{m1} \cos(\omega_0 t) = 0.845 I_m \cos(\omega_0 t - 90^\circ)$$

V_{m1} and I_{m1} are the **peak** voltage and current values at the fundamental frequency, while V_m and I_m are the **peak** values of the **unclipped** voltage and current waveforms. Let P_{avg1} , P_{avg2} , P_{avg3} ... represent the average power flows at fundamental **2nd**, **3rd** ... harmonic frequencies in 'watts'.

$$\begin{aligned} P_{avg1} &= \text{Average} [v_1(t) \cdot i_1(t)] \\ &= 0.357012 V_m \cdot I_m \text{ W} \end{aligned}$$

Similarly,

$$\begin{aligned} P_{avg2} &= \text{average} [v_2(t) \cdot i_2(t)] \\ &= 0.001407 V_m \cdot I_m \end{aligned}$$

$$P_{avg3} = 0.027173 V_m \cdot I_m$$

$$P_{avg4} = 0.000064615 V_m \cdot I_m$$

$$P_{avg5} = 0.00028583 V_m \cdot I_m$$

$$P_{avg6} = 0.000041314 V_m \cdot I_m$$

$$P_{avg7} = 0.002268 V_m \cdot I_m$$

$$P_{avg8} = 0.0000031903 V_m \cdot I_m$$

$$P_{avg9} = 0.00591937 V_m \cdot I_m$$

$$P_{avg10} = 0.00000129122 V_m \cdot I_m$$

$$P_{avg11} = 0.00103717 V_m \cdot I_m$$

$$P_{avg12} = 0.0000024642 V_m \cdot I_m$$

$$P_{avg13} = 0.00076596 V_m \cdot I_m$$

The total average power flowing in the circuit is the sum total of the above individual average harmonic powers.

$$\begin{aligned}
 P_{avg} &= (P_{avg1} + P_{avg2} + P_{avg3} + P_{avg4} + P_{avg5} + P_{avg6} + P_{avg7} + \\
 &\quad P_{avg8} + P_{avg9} + P_{avg10} + P_{avg11} + P_{avg12} + P_{avg13} + \dots) \\
 &= 0.39598 \text{ V}_m * I_m \text{watts} \quad \dots (2.10) \\
 &= \text{Total average power flowing in the circuit as found out by the multiplication} \\
 &\quad \text{of the instantaneous voltage and current.}
 \end{aligned}$$

Thus we see that it is easy to distinguish the contributions of the individual current and voltage harmonics in the total average power. But the same is not true: for the reactive power as the same harmonic components in the voltage and current are not the only contributors to the reactive power component at that frequency. From the present case it is clear that the sum total of the average power can be found out directly from the contributions of each of the voltage and current harmonics. Even though we can easily make out the total reactive power flowing in the circuit it is not easy to get any useful information out of it.

2.3.1 Interpretation of the Analysis of Instantaneous Power

One important observation in the above expression for the average power is the fact that the average power at each and every harmonic frequency is positive. This observation is significant in the respect that it testifies to fact that the direction of flow of power at each and every harmonic frequency is from the source to the load. This **directionality** can be explained by the basics of power flow in a single phase ac circuit, as has been further along in the discussions. Before that let us look at the power flow in a circuit which has a known source of harmonics.

2.4. Analysis of Power Flow in a Circuit with a Nonlinearity

I will like to discuss the case for a flat topped wave, when applied to a diode. The diode is a unidirectional current device, its characteristic is nonlinear. The diode will clip the negative half wave in such a way that the current flows in pulses of **half wave rectified** sine only. Figure 3, which is shown above illustrates this setup conceptually.

With out any loss of generality and for the sake of convenience let us take the flat topped waveform already taken above as an voltage waveform. Again it is given by equation (2.7).

$$v_{ab}(t) = V_m \{ (0.845 \sin(\omega_0 t) + 0.05305 \cos(2\omega_0 t) + 0.23312 \cos(3\omega_0 t + 260.2^\circ) + 0.011368 \cos(4\omega_0 t) + 0.0239096 \cos(5\omega_0 t + 73.9^\circ) + 0.00909 \cos(6\omega_0 t + 180^\circ) + 0.06735 \cos(7\omega_0 t - 87.17^\circ) + 0.002526 \cos(8\omega_0 t) + 0.108806 \cos(9\omega_0 t + 267.91^\circ) + 0.001607 \cos(10\omega_0 t) + 0.0455 \cos(11\omega_0 t - 88.33^\circ) + 0.00222 \cos(12\omega_0 t + 180^\circ) + 0.03914 \cos(13\omega_0 t - 88.63^\circ) + .. \dots \dots \dots \} \dots \dots \dots \quad \dots \quad (2.11)$$

The only assumption here is that the voltage is periodic so that its Fourier coefficients can be found. When such a wave is passed through a diode, the current waveform is now modified. Owing to the nonlinear nature of the diode characteristics it clips the positive half of the voltage waveform. The point to note here is that the current flows in the circuit owing to certain properties of this semiconductor device. Since nonlinearity exists in the load, the current waveform cannot be directly analyzed in terms of the harmonics of the voltage waveform. Unlike the linear cases like resistors where such a constraint is not a problem we have to resort to this constraint in all nonlinear circuits. What it means analytically is that the current harmonics may or may not be exactly dependent on the voltage harmonics. So, in order to find the current harmonics we have to circumvent this

problem and find the current harmonics by having a Fourier series of this **current** waveform separately. All linear circuit analysis techniques will have to be **abandoned** for the moment. The current waveform is decomposed into its harmonic components as was done for the voltage waveform.

The harmonic components of a flat topped half wave-rectified current waveshapes are as given below

$$i_{ab}(t) = I_m * [0.606985 + 0.622008 \cos(\omega_0 t - 90^\circ) + 0.317685 \cos(2\omega_0 t + 114.68^\circ) + 0.497018 \cos(3\omega_0 t + 85.408^\circ) + 0.293 \cos(4\omega_0 t + 99.9^\circ) + 0.21986 \cos(5\omega_0 t - 88.27^\circ) + 0.28925 \cos(6\omega_0 t + 93.61^\circ) + 0.25423 \cos(7\omega_0 t - 89.25^\circ) + 0.2888 \cos(8\omega_0 t + 91.82^\circ) + 0.350722 \cos(9\omega_0 t + 90.65^\circ) + 0.28875 \cos(10\omega_0 t + 91.37^\circ) + 0.26111 \cos(11\omega_0 t - 89.71^\circ) + 0.2887 \cos(12\omega_0 t + 90.88^\circ) + 0.2716 \cos(13\omega_0 t - 81.98^\circ) + \dots \quad \dots \quad (2.12)$$

The point to be noted here, looking at both the voltage and current harmonic components is that the relative magnitudes and phase angles of both the **harmonics** of these waveforms are not directly related in any case.

2.4.1. Calculation of the Instantaneous Power

Now, let us look at the instantaneous power expression once again.

$$P_{ab} = v_{ab}(t) * i_{ab}(t)$$

The instantaneous power expression comes out to be

$$p_{ab} = V_m * I_m * (0.20116199 + 0.3314 \cos(\omega_0 t - 84.23^\circ) + 0.12284 \cos(2\omega_0 t + 164.56^\circ) + 0.17229 \cos(3\omega_0 t + 248.43^\circ) + 0.0736 \cos(4\omega_0 t + 196.45^\circ) + 0.01828 \cos(5\omega_0 t - 6.64^\circ) + 0.042686 \cos(6\omega_0 t - 13.6^\circ) + 0.05142 \cos(7\omega_0 t +$$

$$P_{avg11} = 0.0059444 V_m * I_m$$

$$P_{avg12} = 0.000004915 V_m * I_m$$

$$P_{avg13} = 0.005262418 V_m * I_m$$

As we see, that the average powers for some **harmonic** frequencies are negative indicating that these power **are** flowing back to the source from the load. The net average power over all frequencies shown can be obtained.

$$\begin{aligned} P_{avg} &= (P_{avg1} + P_{avg2} + P_{avg3} + P_{avg4} + P_{avg5} + P_{avg6} + P_{avg7} + \\ &\quad P_{avg8} + P_{avg9} + P_{avg10} + P_{avg11} + P_{avg12} + P_{avg13} + \dots) \\ &= 0.20116199 V_m * I_m \end{aligned}$$

= Total average power flowing in the circuit as found out by the multiplication of the instantaneous voltage and current.

One of the most striking aspects of this analysis is the fact that the average power at certain frequencies is coming out to be negative. In a circuit which has **only** the electrical elements in a system there is no reason for the power at any harmonic frequency to go negative.

The average power flowing at the fundamental frequency is

$$\begin{aligned} P_{avg1} &= \text{average} (v_1(t) * i_1(t)) = V_{m1} \cos(\omega_0 t - 90) * I_{m1} \cos(\omega_0 t - 90) \\ &= V_{m1} * I_{m1} \end{aligned}$$

where V_{mi} , I_{mi} are the peak values of the currents and voltages flowing at the fundamental frequency.

Similarly the average power flow at other frequencies are

$$\begin{aligned} P_{avg2} &= \text{average} (v_2(t) * i_2(t)) \\ &= V_{m2} * I_{m2} * \cos(114.680) \\ &= -0.41755 V_{m2} * I_{m2} \end{aligned}$$

$$\begin{aligned}
 P_{\text{avg}3} &= v_3(t) * i_3(t) \\
 &= V_{m3} * I_{m3} * \cos(174.79^\circ) \\
 &= -0.9958717 V_{m3} * I_{m3}
 \end{aligned}$$

$$\begin{aligned}
 P_{\text{avg}4} &= v_4(t) * i_4(t) \\
 &= V_{m4} * I_{m4} \cos(99.9^\circ) \\
 &= -0.17193 V_{m4} * I_{m4}
 \end{aligned}$$

$$\begin{aligned}
 P_{\text{avg}5} &= \text{average} (v_5(t) * i_5(t)) \\
 &= V_{m5} * I_{m5} \cos(162.17^\circ) \\
 &= -0.95197 V_{m5} * I_{m5}
 \end{aligned}$$

$$\begin{aligned}
 P_{\text{avg}6} &= \text{average} (v_6(t) * i_6(t)) \\
 &= V_{m6} * I_{m6} \cos(86.39^\circ) \\
 &= 0.06296 V_{m6} * I_{m6}
 \end{aligned}$$

2.4.2. Interpretation of the Direction of Average Power Flow in a Nonlinear Circuit

From the previous expressions for the average voltage it can be **easily** seen that the **power** is not unidirectional at all the harmonic frequencies examined. The load is taking power at the fundamental and the fifth harmonic frequency while it is throwing power out on the power system at other harmonic frequencies like the second, third, fourth etc. The **point** to be noticed is that even though the power is negative at certain **harmonic frequencies**, the total power entering the system is positive, that is there is net transfer of **energy** from the source to the load. Thus, it is clearly seen that though the load is consuming energy, yet at the same time the source is acting as a sink for **certain** other harmonics.

A closer examination shows that the relative phase difference between the harmonic **voltage** and current phasors, at different frequencies varies all over the four quadrants. As long as the phase difference between the voltage and current at a particular harmonic is

below 90° the average power flow at that frequency is positive. But as soon as this phase difference becomes more than 90° the average power flow at that particular frequency goes negative.

2.5. Average Power Analysis in Terms of Phasors

It is helpful to view the average power in terms of the phase relation of the harmonic components. For example in the case discussed in Section 2.4, at the fundamental frequency (60Hz), the voltage and current phasors are in **direct** phase with each other.



Figure 4 Fundamental voltage and current phasors for a diode:load

$$\text{Here } \theta_{d1} = \theta_{m1} - \theta'_{m1} = 0$$

where θ_{d1} represents the phase difference between the voltage and current phasors at the fundamental frequency, θ_{m1} and θ'_{m1} represent the actual positions of the voltage and current phasors from the reference point.

At the second harmonic frequency we see,

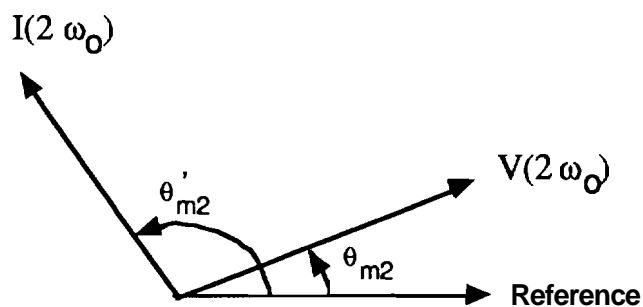


Figure 5 Voltage and current phasors at the second harmonic frequency for the diode load

Here $\theta_{d2} = \theta_{d1} = \theta_{m1} - \theta'_{m1} = 114.680$

At the second harmonic the relative phase angle between the voltage and current is 114.680. This shows a negative power flow at that frequency. In other words, at the second harmonic the source acts as a power sink.

The same inference can be drawn from the third harmonic.

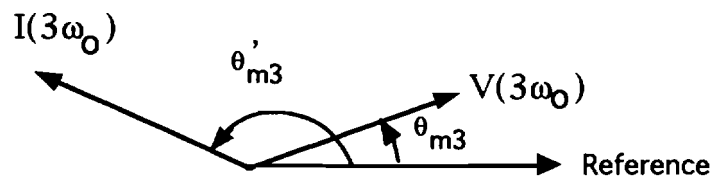


Figure 6 Voltage and current phasors at the third harmonic frequency for the diode load

Here the value of θ_{d3} is 174.790, which again shows negative power flow at this frequency (at 180 Hz).

This reverse flow of average power back to the source from a harmonic load at certain frequencies can be exploited to detect the presence of such kinds of loads on a power system. A close look at average power calculated above shows that the relative phase angle between the voltage and current at each and every harmonic frequency determines whether the power is being taken in by the load at that particular frequency or vice-versa. Note however that the relative phase angle between the input voltage and input current for an RLC load at any frequency is never more than 90° .

The above phase relationship between the voltage and current, for any electrical load (reactive or resistive) holds true at all the frequencies, including at the fundamental and harmonic frequencies separately. The only difference being that the value of load impedance for different frequencies is different.

Since the inductive reactance, X_L is directly proportional to the frequency and Capacitive reactance, X_C , is inversely proportional to the frequency, the relative phase difference between the harmonic voltage and current components of a mixed R L C load will vary with frequency, nevertheless these phase difference will remain between the bound of 90° .

In the case for a diode type of load it is clearly seen that the relative phase difference between the voltages and currents at different frequencies is more than 90° . At some frequencies it less than 90° , while at others it is more than 90° . Now as said above that in an electrical circuit with only R,L,C components this cannot happen, that is the phase angle can never be more than 90° .

Thus from the above discussion it can be safely concluded, that the relative difference in phase angles of the voltages and currents at the harmonic frequency, being more than 90° is a clear indication of the presence of nonlinear loads (harmonic loads) in the circuit. This basis will be used in the present work to distinguish nonlinear harmonic loads from harmonic free electrical loads.

Before I go any further I will like to make a comment on the nature of the present analysis. Analysis of nonlinear circuits is not possible by the use of techniques like Ohm's law, which are used normally for linear devices. This is owing to the fact that with nonlinear devices such as diodes, rectifiers operating in a circuit, the individual harmonic currents no longer have a fixed relationship to the individual harmonic voltages applied to the device. The conduction state of most of the semiconductor devices are: voltage dependent. The distorted voltage determines the time or current at which the diode turns on. Only thereafter does the current start flowing through it. The diode turns off when its current attempts to go negative.

From a different angle of view, each harmonic device by itself leaves a trace of its nonlinear characteristics on its current waveform. This implies that it is possible to

measure the distortion effect of a particular load by looking at the way it **is** distorting its current waveform relative to the applied voltage waveform. And this **observation** should be fully exploited to distinguish harmonic loads from linear electrical loads.

At this point, I will like to define harmonic loads . From the **previous** discussion, two cases will arise in terms of the applied voltage to any device. First, when the voltage **applied** is a pure sinusoid. Second, when the voltage applied is distorted, not a pure sinusoid [1].

2.6. Definition of Harmonic Loads

Case - I When the applied voltage to a load is a pure sinusoid.

If the characteristics of the load are such that on the application of a pure **sinusoidal** voltage, it causes harmonics to appear in the current waveform, then it is a harmonic load.

The nature of current harmonics in such a case will be determined by the nature of the non linearity of the load. A simple Fourier analysis of the current waveform is enough to determine that the load is a harmonic load under this situation.

Case - II When the applied voltage to a load is not a pure sinusoid.

When there are harmonics present in the voltage waveform itself. Then the load is said to be a harmonic load if any of the harmonic power

$$P = \text{Real} (v_n(t) * i_n(t)) < 0 \text{ for integer } n > 1.$$

Where $v_n(t)$ and $i_n(t)$ are the voltage and current at the 'n' th **harmonic**. Harmonic loads can also be defined in terms of the relative phase difference between voltage and **current** phasors at the same frequency. A phase difference of greater than $\pm 90^\circ$ indicates a

harmonic load. This condition of variable relative phase difference between the voltage and current phasor is represented graphically in Figure 7. This figure holds **only** for frequencies greater than the fundamental frequency. This is on account of the fact that **harmonic** distortion occurs only with the presence of frequencies greater than the **fundamental** frequency. A negative real power at the fundamental frequency simply indicates the presence of an active load on the system.

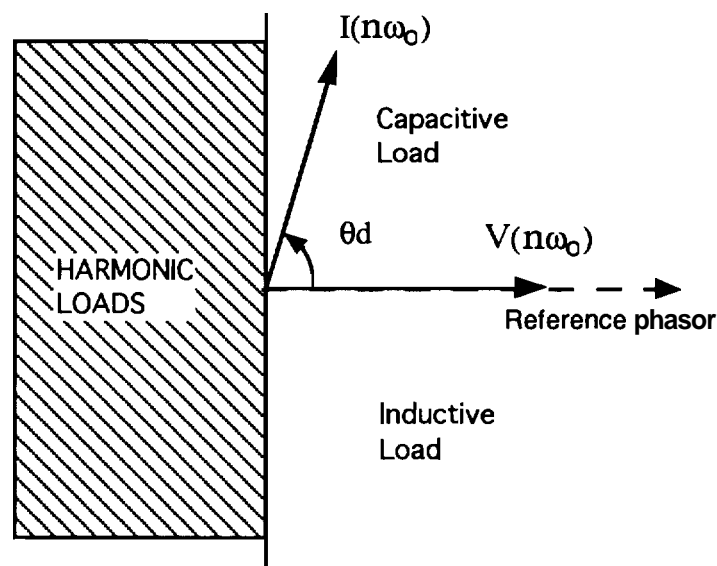


Figure 7. Domains of the current phasor for capacitive, **inductive** and harmonic loads

2.7. Definition of Distortion

For future reference I will like to define distortion as a variation in the shape of current waveform as compared to the shape of voltage waveform. There is a tricky point to be noted here. When a **non-sinusoidal** periodic voltage is applied to a **capacitive** or an inductive circuit, the reactance value of the capacitor or inductor is different for the different frequencies. As a result the relative magnitude and phase shift between the voltage and

currents phasors at different frequencies **will** be different. The apparent effect is a noticeable distortion in the current waveshape in comparison to the **applied** voltage waveshape. But such distortions are not an indication of that the load is a harmonic load. The point made out is that capacitive and inductive loads can cause a distortion of the kind mentioned but they are not considered as harmonic loads.

CHAPTER 3. EXPERIMENTAL SET UP AND DETAILS

3.1. Details of the Experimental Set up and Components

Experimental data on various kinds of electrical loads were collected using a PC based data acquisition system. The set up consisted of current measuring and voltage measuring isolation amplifiers, analog to digital conversion board, **simultaneous** sample and hold board and a Personal Computer. The complete experimental set up for this system is shown in Figure 8.

A CIO-AD16JR-AT analog to digital conversion board manufactured by Computer Boards Inc, was used for digitizing the analog voltage and current **waveforms**. This board has a capacity for 8 differential ended inputs at a given time. It gives 12 bits of resolution with an accuracy of ± 1 bit (0.01% of the reading). It can go **upto** a **maximum** frequency of 330 **kHz**, single channel.

To get the voltage and current waveforms simultaneously a **simultaneous** sample and hold board CIO-SSH16, again manufactured by Computer Boards Inc, has been used. This board can take in 16 differential channels with an accuracy of ± 1 bit. The common mode rejection ratio is greater than 90 dB for all ranges. An LF398 S&H chip and an INA110 differential amplifier has been used on this board. The **maximum** aperture time is 250 **nS** and typical aperture uncertainty is quoted as 50 **nS**. The **maximum** acquisition time is 10 **micro** second, and the droop rate is $\pm 100 \mu\text{V/ms}$. The purpose of **having** this board is **to** be able to gather the voltage and current data simultaneously with **minimum** skew to reduce phase errors between the two set of data. To the front end of this **SSH** board are connected current and voltage isolation amplifiers, which provide **electrical** isolation

between the actual load under test and the PC based experimental set up. **These** amplifiers have adjustable gain ratios. **Maximum** voltage level to the voltage **amplifier** is 5 volts, and current amplifier is 50 mV respectively.

3.2. Analysis of the Acquired Data

The acquired data are stored on the hard disk of the PC, from which they could be retrieved for later processing. The Fast Fourier Transform (FFT) is used to find the magnitude and phase of the harmonic components in the **current** and voltage waveforms **separately**. The output from the FFT are then used to determine the flow of power at each and every harmonic component.

In order to get the correct information out of FFT technique it is **worthwhile** to understand what is involved in an FFT analysis. In particular errors from spectral leakage and picket fencing effect could affect the accuracy of the data under test. There are certain ways to reduce these errors which should be adhered to while using the FFT analysis software. One of the important consideration is the number of cycles of data on which this FFT analysis is applied. To minimized the spectral leakage and picket **fence** effects the number of cycles of voltage and **current** data should be integral. The ill-effect of not keeping the number of data cycles integral was observed during the analysis of the acquired data. If the number of the data cycles is not integral then the harmonic **peaks** will not fall on **frequencies** which are exact multiples of the fundamental. Such a situation will give incorrect magnitude and phase angles of the data under test. It should be **avoided** by truncating the data in such a way that the digitized data represents the data from an integral number of voltage or current waveform cycles.

However before **proceeding** onto such details of the FFT analysis I will like to discuss the results from two experimental cases which substantiate the theoretical analysis presented here. Experiments were done on a variety of loads ranging from incandescent

lamp, ballast fluorescent lamp, variable speed PWM motor drives, triac operated light dimmer mechanism to induction arc welding equipment. For the sake of convenience I have presented results from only two of these experimental loads. The first case is an example of a semiconductor type load of computer monitor. The second case, that of a compact fluorescent lamp is an example of magnetic / plasma nonlinearity [9].

3.3. Experiment 1: A Computer Monitor Load

The experiment was performed on a Panasonic Model No. C1381 computer monitor. This monitor uses a PWM switching converter as a power supply in its internal circuitry.

The monitor is used as the load under test as shown in the experimental setup of Figure 8. The input voltage and the current to the monitor are shown in the figure 10. The current and voltage waveforms were sampled at 50,000 Hz, and 25,000 samples of each were taken. Then Fast Fourier Transform was applied to the data obtained and the results for the voltage and current waveforms, are shown in Figures 11 and 12, respectively. The magnitude of voltage and current harmonic components as determined by sorting through the peaks of the FFT results are in Table 1. The individual voltage component values are in volts and the phase angles are in radians.

Table 1. FFT Analysis of the Voltage and Current Drawn by the Computer Monitor

Frequency	Harmonic Voltage 'volts'	Voltage Phase angle in radians	Harmonic Current 'Amps'	Current phase angle in radians
60 Hz.	164.08	1.9166	0.73988	1.8855
120 Hz.	0.24602	-2.2995	1.08e-03	2.7571
180 Hz.	2.4204	-2.6124	0.57756	-0.7261
240 Hz.	negligible	0	negligible	0
300 Hz.	6.44008	0.2419	0.34866	2.9311
360 Hz.	negligible	0	negligible	0
420 Hz.	1.43944	-2.2502	0.12540	0.1871
480 Hz.	negligible	0	negligible	0
540 Hz.	1.03632	-0.9834	0.05066	1.7124
600 Hz.	negligible	0	negligible	0
660 Hz.	0.32842	1.5583	0.10308	-1.2749
720 Hz.	0.03796	2.9394	9.8e-04	0.3295
780 Hz.	0.22422	-2.0779	0.0812	2.3721
840 Hz.	0.03942	-1.8509	1.646e-03	-1.9895
900 Hz.	0.22586	-0.5772	0.0238	-0.2422
960 Hz.	0.01816	0.3184	1.88e-03	1.966
1020 Hz.	0.15208	0.5825	0.0258	0.393
1080 Hz.	0.0183	2.8651	1.72e-03	-0.1268
1140 Hz.	0.09684	2.8826	0.0426	-2.2749

Table 1, Continued

1200 Hz.	0.04122	-2.3319	2.04e-03	-1.9596
1260 Hz.	0.18448	-1.189	0.02906	1.2580
1320 Hz.	0.02308	-2.5718	2.252e-03	2.1991
1380 Hz.	0.13022	-0.8426	7.916e-03	-2.2308
1440 Hz.	0.01878	2.8772	2.69e-03	-0.0665
1500 Hz.	0.05268	-1.9039	0.014032	-0.0916

3.3.1. Determination of Direction of Average Power Flow

To determine the direction of average power flow at every harmonic frequency it is **necessary** to use the current and voltage components found above at each **and** every harmonic.

The active power at any frequency is given as

$$P = V_{rms} * I_{rms} * \text{power factor}$$

$$= V_{rms} * I_{rms} * \cos(\theta - \theta' - \theta_{err})$$

where $(\theta - \theta' - \theta_{err})$ is the relative phase difference between the voltage **and** current phasor. θ_{err} represents the phase difference between the voltage and **current** channels of the **data** acquisition system. It can be determined from the difference in the phase angle vs frequency characteristics of the voltage and current amplifiers. It varies from 0° to at the most **60**, over the frequency range from **0** to **1500 Hz**.

The average power of the 'i' th harmonic can then be computed from

$$P_i = (V_{mi} * I_{mi}) / 2 * \cos(\theta_{mi} - \theta'_{mi} - \theta_{erri})$$

for i = 1,2,3

For example, that of the fundamental is

$$\begin{aligned}
P_1 &= (V_{m1} * I_{m1}) / 2 * \cos(\theta_{m1} - \theta'_{m1} - \theta_{err1}) \\
&= (164.08 * 0.73988) / 2 * \cos(1.78^\circ) \\
&= 60.670464 \text{ W}
\end{aligned}$$

and those for the higher components are

$$\begin{aligned}
P_2 &= 4.48 \text{ e-}05 \\
P_3 &= -0.21688 \\
P_4 &= \text{None} \\
P_5 &= -0.982692 \\
P_6 &= \text{None} \\
P_7 &= -0.064566 \\
P_8 &= \text{None} \\
P_9 &= -0.023275 \\
P_{10} &= \text{None} \\
P_{11} &= -0.016039 \\
P_{12} &= -1.569372\text{e-}05 \\
P_{13} &= -2.514\text{e-}03 \\
P_{14} &= 3.22049\text{e-}05 \\
P_{15} &= 2.5811\text{e-}03 \\
P_{16} &= 0.00 \\
P_{17} &= 1.952\text{e-}03 \\
P_{18} &= -1.5159\text{e-}05 \\
P_{19} &= 6.8864\text{e-}04 \\
P_{20} &= 4.013552\text{e-}05 \\
P_{21} &= -1.902092\text{e-}03 \\
P_{22} &= 1.200448\text{e-}06 \\
P_{23} &= 1.28716\text{e-}04
\end{aligned}$$

$$P_{24} = -2.4239e-05$$

$$P_{25} = -5.03982e-05$$

Note that the direction of power flow in the third and some other harmonics is negative, opposite to the direction of power flow in the fundamental frequency.

3.3.2. Interpretation of the Results for Experiment 1

In the above analysis for power flow, the magnitude of the power flow at any **harmonic** is not so important as its direction. As seen above the power flow is negative in the **3rd, 5th, 7th, 9th, 11th, 12th, 13th, 16th, 18th, 21st, 24th and 25 th harmonics**.

The computer monitor by our definition a harmonic load.

3.4. Applicability of the Method to Other Nonlinear Harmonic Loads

The above analogy has been shown to work on semi-conductor loads. I will like to make my point about nonlinearities in general and show that this analysis works for any **kind** of nonlinearity. I will like to generalize it to the fact that any **nonlinear** load will give out negative average power at harmonic frequencies and such a nonlinearity can be detected by the proposed method. This is due to the fact that any kind of periodic **signal** can be decomposed into its Fourier components and the same analysis can be **performed** on it.

As a second experiment I will like to bring in the case of a fluorescent lamp load. Fluorescent lamps **are** also a source of harmonics on the power system [9], even though they may not have semiconductor devices.

3.5. Experiment 2: A Fluorescent Lamp Load

The compact fluorescent lamp under investigation is a **Sylvania** Cool White lamp, with **model** no: **FC8T9-CW-R5**. The voltage applied to the lamp and the **current** drawn by it are shown in Figure 13. The harmonic component magnitudes from the FFT plots of the

voltage and current waveforms are shown in Fig. 14 and 15. In the Table 2 below, V_{mi} and I_{mi} represent the peak values of the i th harmonic component.

Table 2. FFT Analysis of the Voltage and Current Drawn by a 40W Fluorescent Lamp

Frequency	Harmonic	Voltage Phase	Harmonic	Current Phase
	Voltage 'volts'	Angle 'radians'	Current 'Amps'	Angle 'radians'
60 Hz.	164.49	1.3794	0.43802	0.4230
120 Hz.	0.4676	2.8136	3.542e-3	3.0618
180 Hz.	2.455	1.9390	0.039716	0.3223
240 Hz.	0.06858	-2.1951	9.86e-04	1.0268
300 Hz.	6.2434	-2.392	9.144e-03	-2.4330
360 Hz.	0.04622	-0.0112	9.36e-04	-1.1198
420 Hz.	1.59162	0.3084	4.88e-03	2.4453
480 Hz.	0.10732	0.7375	3.52e-04	2.9651
540 Hz.	1.06866	0.5719	2.322e-03	0.2268
600 Hz.	0.08132	1.3056	4.54e-04	0.2997
660 Hz.	0.53982	2.4269	1.3e-03	-1.8606
720 Hz.	0.44664	2.5726	3e-04	1.4524
780 Hz.	0.30938	-2.8392	9.24e-04	2.3771
840 Hz.	0.03778	-2.8887	2.2e-04	2.2601
900 Hz.	0.18774	-2.0262	5.4e-04	0.0410
960 Hz.	9.02e-03	-2.2098	1.52e-04	0.1791
1020 Hz.	0.1763	-2.4251	4.8e-04	-2.4253

Table 2, Continued

1080 Hz.	0.02574	-1.3338	7.2e-05	-2.1314
1140 Hz.	0.09982	-1.5076	3.2e-04	1.5944
1200 Hz.	0.02348	-0.6087	1.8e-04	1.6373
1260 Hz.	0.14446	-0.2643	2.96e-04	-0.8223
1320 Hz.	0.03054	-2.0580	1.04e-04	-0.3921
1380 Hz.	0.1481	-0.6320	2.52e-04	2.9544
1440 Hz.	0.04244	-2.5878	1.14e-04	-2.6619
1500 Hz.	0.28848	-2.0786	2.6e-04	0.663

3.5.1. Determination of the Direction of the Active Power

At any frequency the active power is given as [6]:

$$P = V_{rms} * I_{rms} * \text{power factor}$$

$$= V_{rms} * I_{rms} * \cos (\theta - \theta' - \theta_{err})$$

where $(\theta - \theta' - \theta_{err})$ is the relative phase difference between the voltage and current phasor and ' θ_{err} ' is the error in relative phase difference due to difference in the phase characteristics of the voltage and current isolation amplifiers. ' θ_{err} ' is zero at most of the frequencies, and it has a finite value only at some of the frequencies. For our case the average power is given as

$$P_i = (V_{mi} * I_{mi}) / 2 * \cos (\theta_{mi} - \theta'_{mi} - \theta_{erri})$$

for $i = 1, 2, 3, \dots$

Now to look at the individual harmonic power flows,

$$\begin{aligned} P_1 &= (V_{m1} * I_{m1}) / 2 * \cos (\theta_{m1} - \theta'_{m1}) \\ &= (164.49 * 0.43802) / 2 * \cos (54.790) \\ &= 41.54216 \end{aligned}$$

Similarly,

$$P_2 = 8.04e-04 \text{ W}$$

$$P_3 = -4.72e-03$$

$$P_4 = -6.76e-05$$

$$P_5 = 5.84e-03$$

$$P_6 = 2.1292e-05$$

$$P_7 = -3.698e-03$$

$$P_8 = -2.254e-05$$

$$P_9 = 2.36304e-03$$

$$P_{10} = 2.0842e-05$$

$$P_{11} = -3.00456e-04$$

$$P_{12} = -6.2684e-05$$

$$P_{13} = 1.33632e-04$$

$$P_{14} = 3.3806e-06$$

$$P_{15} = -4.3549e-05$$

$$P_{16} = -9.3276e-07$$

$$P_{17} = 8.4096e-05$$

$$P_{18} = 1.44656e-06$$

$$P_{19} = -3.161024e-05$$

$$P_{20} = -1.44288e-06$$

$$P_{21} = 3.81096e-05$$

$$P_{22} = 0.00 \text{ watts}$$

$$P_{23} = -3.47292e-05$$

$$P_{24} = 5.8516e-05$$

$$P_{25} = -6.5648e-05$$

The average power flow of the 3rd, 4th, 7th, 8th, 11th, 12th, 15th, 16th, 19th, 20th, 23rd and 25th harmonics is negative. This correctly identifies the compact fluorescent lamp as a **harmonic** load.

3.6. Details of Experimentation and Analysis

As has been shown previously that we have to **find** out the individual harmonic components in the voltage and current to be able to determine the average (real) power flow at a particular frequency. There are certain precautions which have to be **taken** to be able to take all the measurements with accuracy. This involves a thorough knowledge of the sampling schemes, limitation of the equipment involved, knowledge of the proper use of the **Fast** Fourier Transform and correct interpretation of the results.

Let me start with the analog to digital conversion process first. To digitize the data we have to sample the data at a certain frequency and get the digitized value at discrete **times**, in such a way that an ambiguous reconstruction of the signal is **not** possible. There is a **maximum** frequency f_N in the signal called the folding or the **Nyquist** frequency, and it is defined as a upper frequency limit to the sampled data, above which an ambiguous reconstruction of the signal is not possible with a given sampling rate. Then sampling theorem says that to preserve the information in a sampled version of this signal, it must be sampled at a rate f_S , such that $f_S \geq 2f_N$. This problem involved in A to D conversion of data is called aliasing, which means that the same set of sampled data points can describe a **number** of time series histories which are indistinguishable to the digital **computer**. This problem of aliasing will not occur if $f_S \geq 2f_N$.

When the sampling rate is not high enough, analog signal has to be passed through a low pass filter before sampling it so that its higher frequency components are suppressed from the sampled data, and condition of the Sampling Theorem is maintained. For all my

experimental purposes I have kept the sampling frequency sufficiently high so that this problem of aliasing will not occur. Assuming that any significant harmonic in a power system will not be beyond the 50th harmonic, it means that the sampling speed should be greater than at least 6000 Hz. In all my measurements the sampling speed is many times larger than this number, as such the effects of aliasing **are** negligible.

Since the analog signal can assume an infinite number of states while the number of bits in a digital representation is limited, quantization **errors** will always occur. The effect of the quantization can be reduced by having more binary states **available** to represent the actual analog signal. With the use of a 12 bit A-D convertor the quantization error is 0.01% which translates to 0.5 mV on full scale and 0.05 mA on full scale on the voltage and current channel, respectively. Looking back to Table 1 and 2 the **harmonic** currents and voltages though small are nevertheless at least an order more these **value**.

As mentioned before that I am using the Fast Fourier Transform (FFT) for the harmonic analysis. FFT is based on the Discrete Fourier Transform (DFT). The mathematical details of DFT are presented in Chapter 4. But, in this section I will like to briefly discuss some of the limitations, and the problems associated with the improper use of the FFT. In practical applications we have to truncate the infinite data length to some finite interval. This truncation results in the windowing effect on the data, where the finite record available can be considered equivalent to the result of multiplying an infinite extent of the data with a finite rectangular window. This gives rise to the spectral leakage effect. Along with the main lobe, containing the desired information, there **are** also some side lobes, which represent the distribution of the energy. These lobes can be reduced by using various windowing techniques, like Hamming and Hanning windows, **available** in Digital Signal Processing. Similarly the number of cycles of the sampled data plays an important **part** in its correct analysis. For sinusoids we must have an integral **number** of cycles for the correct FFT analysis of data. If it is not the case, then the picket fence effect becomes

predominant. In cases where the sampled data does not represent an integral number of cycles then it should be truncated accordingly to do so. Both the spectral leakage and picket fence effect are explained in detail in Chapter 4.

3.6.1 Inadequacy of the Cross-Spectrum of the Instantaneous Power

Some researchers previously used the cross-spectrum of the voltage and current (instantaneous power) to determine the direction of the power flow at a particular harmonic. A Cross-spectrum of the voltage and current waveforms in time domain **yields** the instantaneous power flow from which the net average power and net reactive power flow can be obtained. As shown in section 2.3, with the non-sinusoidal supply voltages non-zero harmonic power flow does not necessarily indicate a harmonic load nor is reactive power flow very helpful in this regard. Thus the use of cross spectrum is not helpful in getting the necessary information.

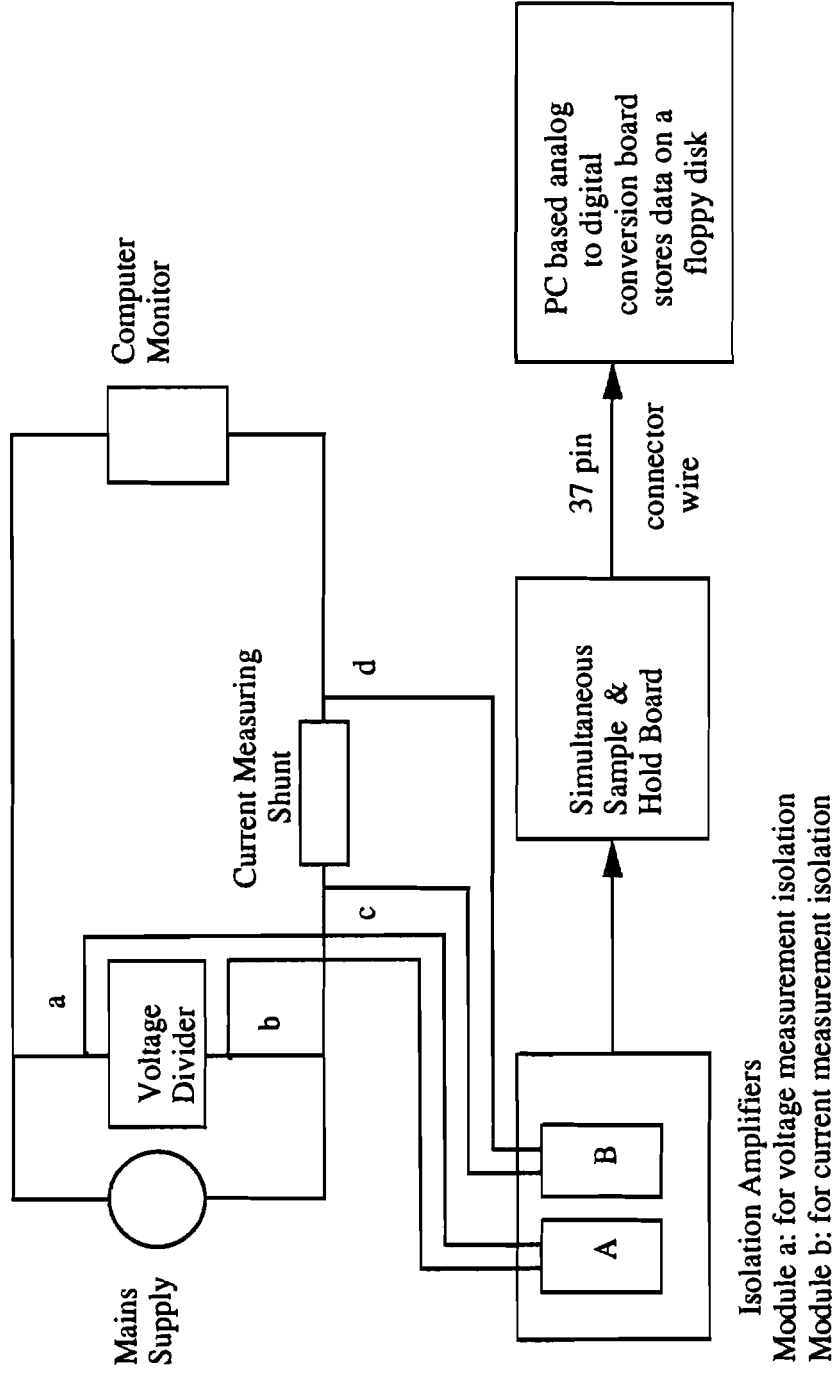


Figure 8. Experimental set-up for voltage and current data acquisition for the computer monitor as the load

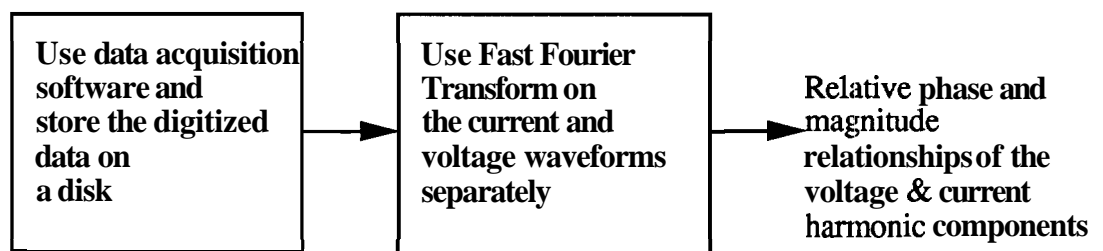
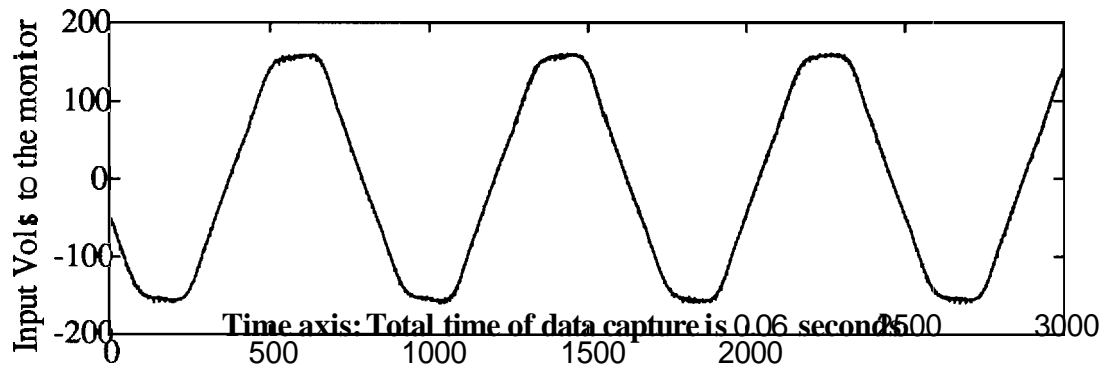
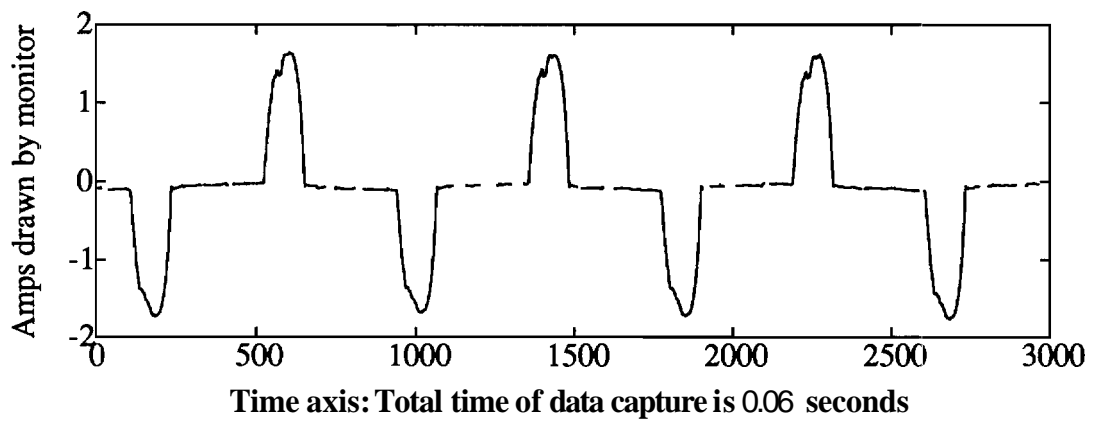


Figure 9. Analysis of the experimentally acquired data

(a)



(b)



**Figure 10. Measured waveforms of the computer monitor(a) Voltage applied
(b) Current drawn**

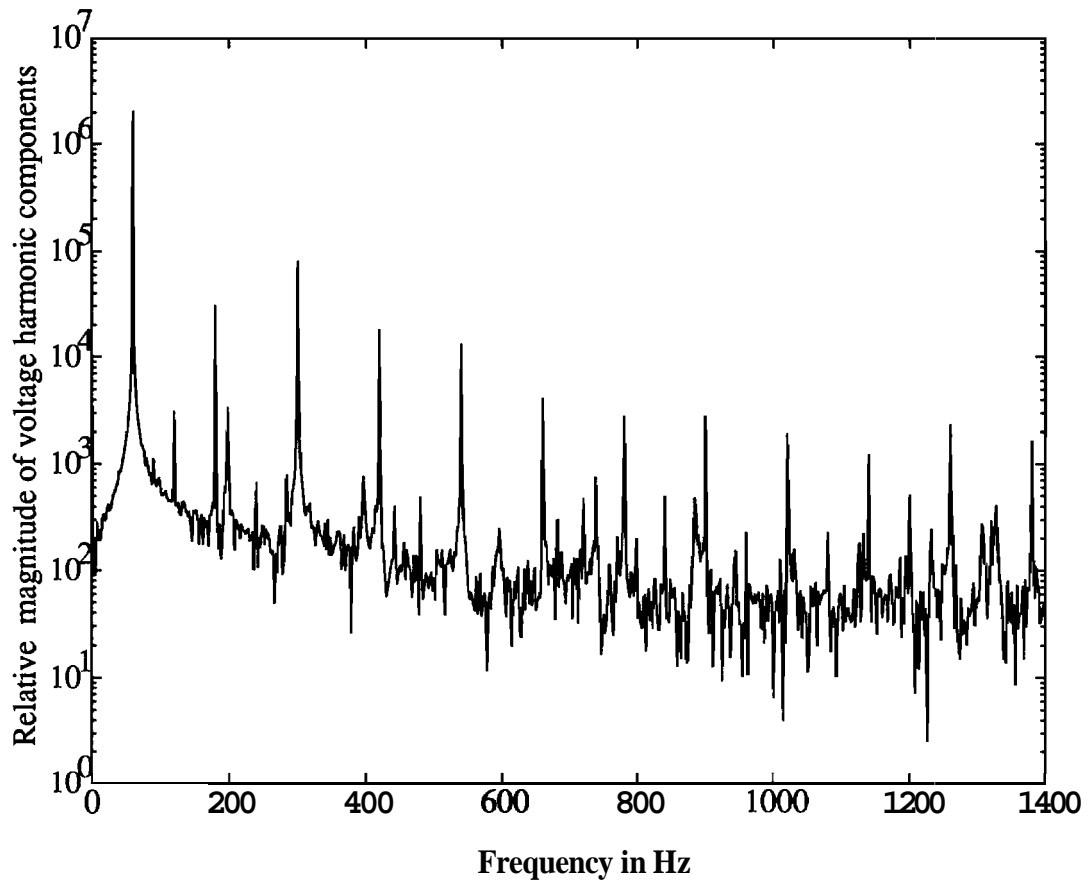


Figure 11. Harmonic components of the voltage waveform fed to the computer monitor

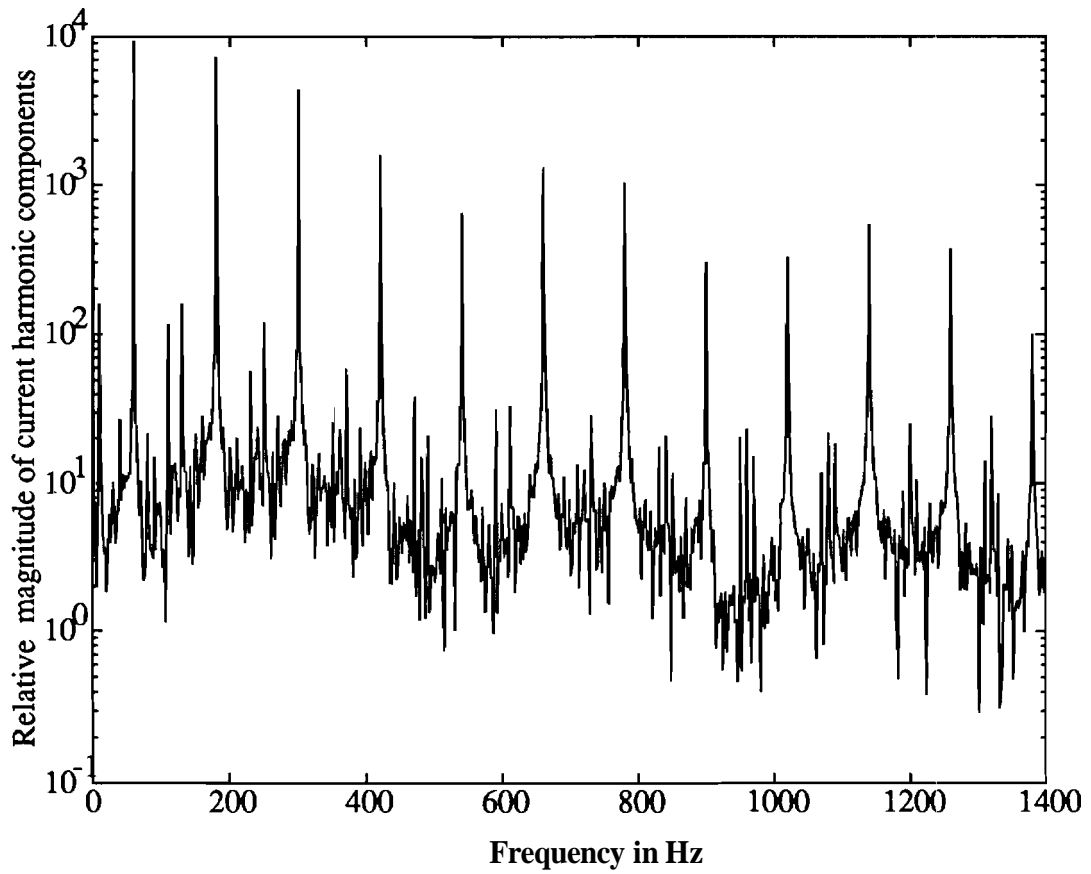


Figure 12. Harmonic components of the current drawn by the computer monitor

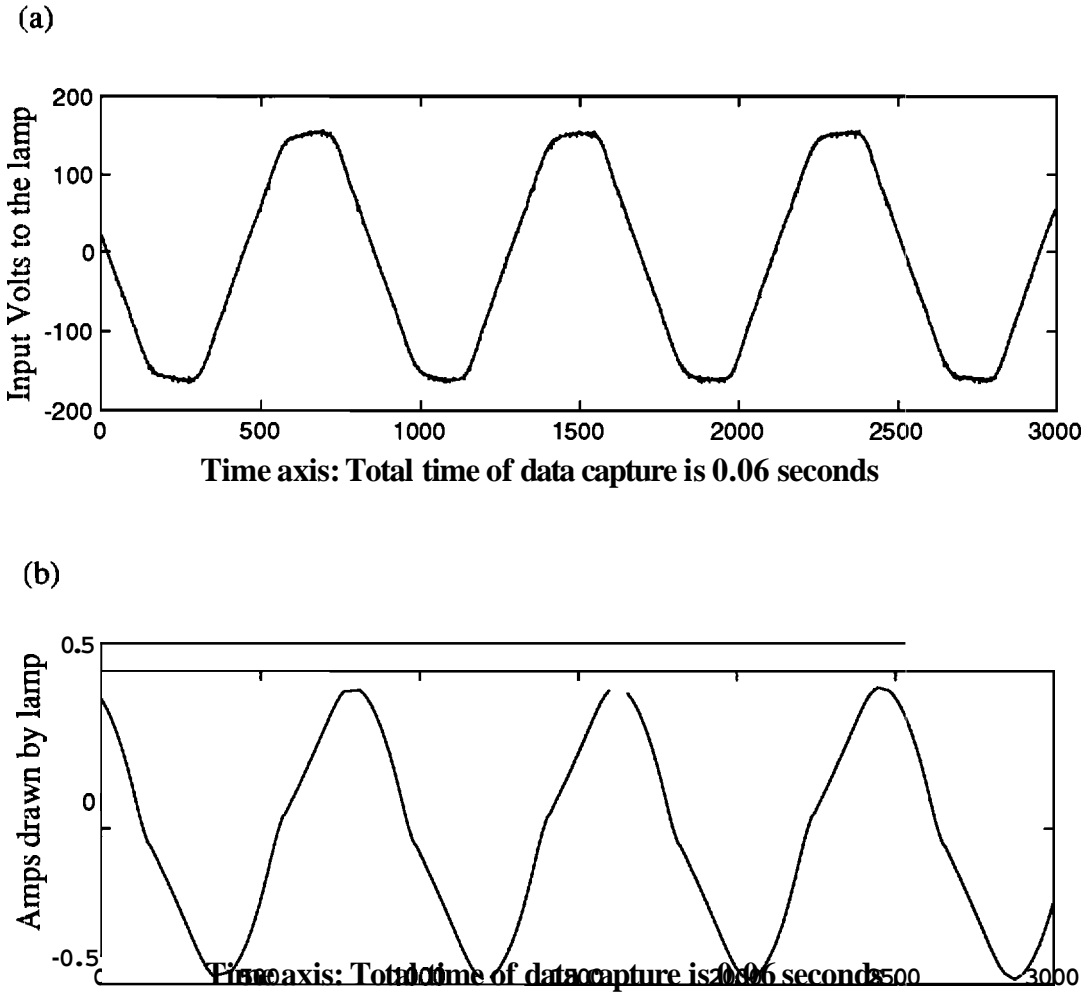


Figure 13. Measured waveforms of the fluorescent lamp (a) Voltage applied
(b) Current drawn

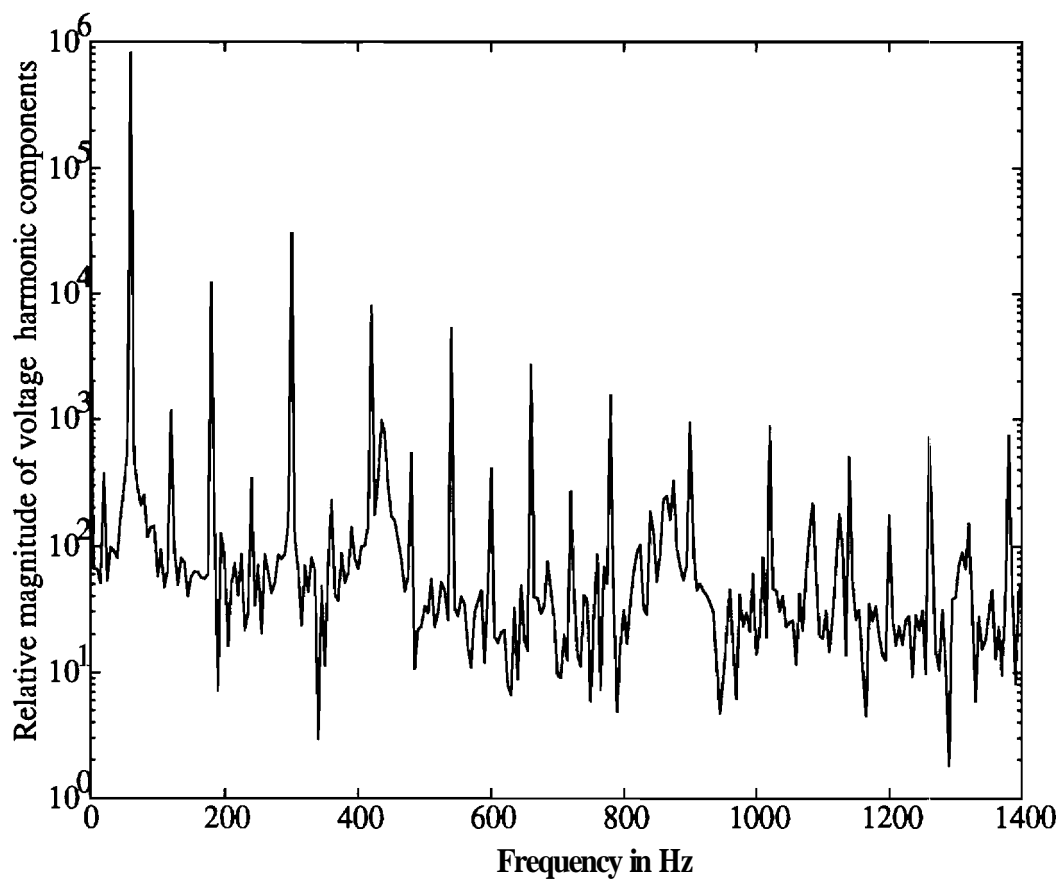


Figure 14. Harmonic components of the voltage fed to the fluorescent lamp

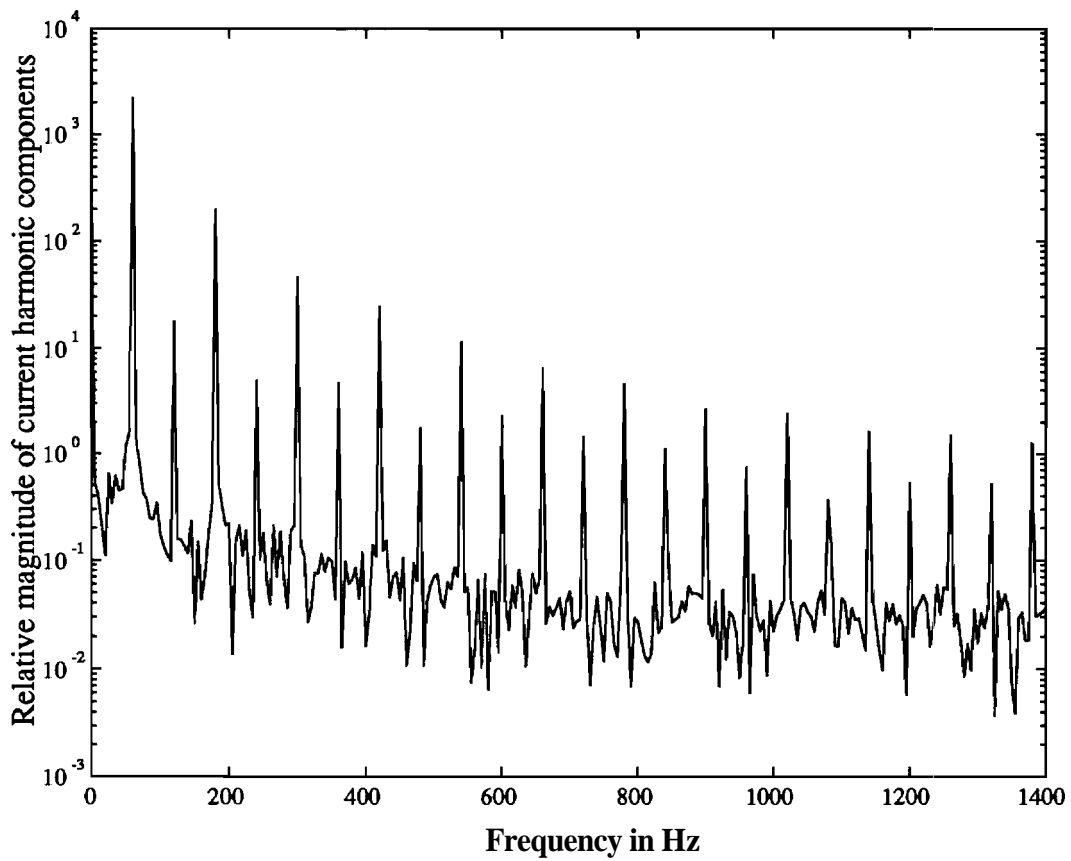


Figure 15. Harmonic components of the current drawn by the fluorescent lamp

CHAPTER 4 FAST FOURIER TRANSFORM AND ITS PROPERTIES

In this chapter some of salient features of FFT and its properties **are** to be reviewed. Where relevant to the accuracy of the proposed method, comments are **added**.

4.1. Properties of Fast Fourier Transform

Let $v(t)$ be a real valued and periodic function with period T . The **complex** coefficients of its Fourier series are given by

$$V_n = \frac{1}{T} \int_0^T v(t) e^{-i \frac{2\pi n t}{T}} dt \quad \dots (4.1)$$

When $v(t)$ is integrable over a period, these coefficients are known to exist.

Under conditions of periodicity, $v(t)$ can be expressed in terms of its Fourier components as

$$\begin{aligned} v(t) &= \sum_n V_n e^{i \frac{2\pi n}{T} t} \\ &= \sum_n V_n e^{i \omega n t} \end{aligned} \quad \dots (4.2)$$

where $\omega = \frac{2\pi}{T}$

If $v(t)$ is sampled and digitized using a sampling period of T_s , then the sampled signal is given as obtain

$$v_k = v(kT_s), \quad \text{for } k \in Z \quad \dots (4.3)$$

where Z is sample set within the finite length window. The windowed function can be written as

$$w_k = \begin{cases} 1, & 0 \leq k \leq N-1 \\ 0, & \text{else} \end{cases} \quad \dots (4.4)$$

where N is the total number of data points of the windowed signal.

Applying this window function to the signal v_k , the windowed signal can be expressed as

$$\tilde{v}_k = v_k w_k = \begin{cases} v_k, & 0 \leq k \leq N-1 \\ 0, & \text{else} \end{cases} \quad \dots (4.5)$$

Taking the discrete time Fourier transform of the windowed function, we get its Fourier coefficients

$$\tilde{V}(\omega) = \sum_{k=0}^{\infty} \tilde{v}_k e^{-i\omega k} = \sum_{k=0}^{N-1} v_k e^{-i\omega k}$$

(Using equation 4.5)

$$\begin{aligned} &= \sum_{k=0}^{N-1} \left(\sum_n v_n e^{i \frac{2\pi n k T_s}{T}} \right) e^{-i\omega k} \\ &= \sum_n v_n \sum_{k=0}^{N-1} e^{i\omega_0 n k} e^{-i\omega k} \end{aligned}$$

Let us define

$$2\pi \left(\frac{T_s}{T} \right) = \omega_0 \quad \dots (4.6)$$

As will be shown later that this constant ω_0 is the fundamental frequency where the main lobe in the window transform is present.

The windowed function is now given as

$$\tilde{V}(\omega) = \sum_n V_n \sum_{k=0}^{N-1} e^{-i(\omega - n\omega_0)k} \quad \dots (4.7)$$

Now two conditions arise for this windowed function as shown in equation 4.8 below.

When the variable ω is an integral multiple of the constant and when it is not.

Or in other words

$$\tilde{V}(\omega) = \sum_{n=-\infty}^{\infty} V_n P(\omega - n\omega_0) \quad \dots (4.8)$$

holds for the case when $\omega \neq n\omega_0$.

$P(\omega)$ is defined as

$$P(\omega) = e^{-\frac{N-1}{2}\omega} \frac{\sin(\frac{N\omega}{2})}{\sin(\frac{\omega}{2})} \quad \dots (4.9)$$

Equation 4.10 as shown above represents the transform of the rectangular window. As can be seen now that the constant ω_0 represents the first main lobe of the **frequency** transformed function. The side lobes of this transformation will cross the X axis at frequencies which are a direct multiple of this frequency ω_0 . This condition is shown in Figure 16, where the main lobe is formed at point b. The other points **c,d,e ...** are multiples of the frequency at b.

Here are some brief aspects of the Discrete Time Fourier **Transform**

- o With real data we are limited to a finite time interval only.
- o Discrete Fourier Transform is nothing more than discrete samples of the DTFT of a finite length sequence.



4.2. Errors Involved in FFT

In communications we are generally interested in detecting isolated frequency components in a signal. But for the purpose of this thesis we are **looking** for the harmonic analysis aspect of this signal detection. In this case the signals to be are a **multiple** of the fundamental frequency. The ability of the DFT to perform this detection in case of **periodic** signals is limited by two error effects.

- o Truncation -**leakage** effect
- o Frequency Sampling (Picket Fence Effect)

4.2.1 Spectral Leakage Errors in FFT'

As has been shown above in equation. (4.9), the windowed signal is given as $\tilde{V}(\omega)$. This expression can be written as a ratio of two **sinc** functions. This magnitude being given as

$$|\tilde{V}(\omega)| = N \left| \frac{\sin c\left(\frac{\omega N}{2}\right)}{\sin c\left(\frac{\omega}{2}\right)} \right| \quad \dots (4.10)$$

$$\approx N \cdot \left| \text{sinc}\left(\frac{\omega N}{2}\right) \right| \quad \dots (4.11)$$

for small values of ω

Now let us take a case where the **discretized** signal can be represented as

$$v_k = \begin{cases} \cos(\omega_0 t) & \dots\dots\dots 0 \leq t \leq NT \\ 0 & \dots\dots\dots \text{else} \end{cases} \quad \dots (4.12)$$

The windowed function for this signal is given by

$$\tilde{v}(t) = w_k \cos(\omega_0 t)$$

where the term w_k is the **windowing** function.

Applying circular convolution, we have the discrete time Fourier **transform** for this signal as

$$\begin{aligned}
 X(\omega) &= \frac{1}{2\pi} \int_{-\pi}^{\pi} P(e^{j(\omega - \mu)}) * \pi[\delta(\mu - \omega_0) + \delta(\mu + \omega_0)] d\mu \\
 &= \frac{1}{2} [P(e^{j(\omega - \omega_0)}) + P(e^{j(\omega + \omega_0)})] \quad \dots (4.13)
 \end{aligned}$$

This is because of the fact that
 $\delta(\mu - \omega_0) \neq 0, \dots \dots \dots \text{for } (\mu = \omega_0), \text{ only}$
 $\delta(\mu + \omega_0) \neq 0, \dots \dots \dots \text{for } (\mu = -\omega_0), \text{ only}$

Instead of the ideal case where energy is present at a single frequency only, we have the case where side lobes are being formed along with the main lobes. Also the width of the main lobe is given by π / N . This spread of the main lobe represents the distribution of energy at other frequencies along with the actual frequency, which is given by the **peak** of the main lobe. The amplitude of the first side lobe is nearly equal to **21.2%** of the main amplitude of the main lobe.

The main problems caused by the leakage is that it we cannot distinguish between two strong frequencies closer than a frequency of

$$\Delta\omega = \frac{2\pi}{N}$$

Secondly we cannot identify a weak frequency component in the vicinity of a strong one. The above mentioned two problems are not relevant to our particular case since the harmonic frequencies are placed far apart. The position of minimum **leakage** is shown in Figure 16.

4.2.2. Picket Fence Effect

As we already know that the Discrete Fourier Transform generates **samples** of Discrete Time Fourier Transform at frequencies of

$$\omega_k = \frac{2\pi k}{N}$$

Now substituting the value of $P(\omega)$ from equation (4.10) into equation (4.13), we get

$$X(\omega) = \left[\frac{1}{2} e^{-j(\omega - \omega_o) \frac{N-1}{2}} \frac{\sin\left[\frac{(\omega - \omega_o)N}{2}\right]}{\sin\left(\frac{\omega - \omega_o}{2}\right)} \right] + \left[\frac{1}{2} e^{-j(\omega + \omega_o) \frac{N-1}{2}} \frac{\sin\left[\frac{(\omega + \omega_o)N}{2}\right]}{\sin\left(\frac{\omega + \omega_o}{2}\right)} \right]$$

Now two types of data arise which show the two extremes of the nature of the picket fence effect

Case I When there is a periodic extension of data, beyond the first cycle.

that is the data length N represents data from an integral number of data cycles.

$$\text{At } \omega = \frac{2\pi k_o}{N},$$

where k_o is the frequency at which the main lobe occurs.

The magnitude of the discrete time Fourier transform at the k th discrete point is given as

$$X_N(k) = \begin{cases} \frac{N}{2}, & k = k_o, N - k_o \\ 0, & \text{else} \end{cases}$$

Thus we see that when the signal is given to this rectangular window, we see lobes at two points. The second lobe is the exact replica of the first one and it occurs at the $(N - k_o)$ th discrete point. The actual signal magnitude at each of these points is multiplied by $N/2$. The same case appears during the actual mathematical analysis of the stored data.

The FFT output from the frequencies 0 to Nyquist folding frequency is repeated from the

Nyquist folding **upto** the frequency at the Nth data point. Thus effectively we are getting the FFT results from the first half of the N data points only. The magnitude of the signals at each of the **harmonic** frequencies is multiplied by **N/2** in the actual FFT vector.

Now,

$$\begin{aligned}\cos(\omega_0 n) &= \cos(\omega_0 (n + N)) \\ &= \cos\left[\frac{2\pi k_0}{N}(n + N)\right] = \cos\left[\frac{2\pi k_0}{N}n\right] \\ &= \cos(\omega_0 n)\end{aligned}$$

Thus we see that the periodic extension of data leads to complete cosine and the **errors** resulting out of picket fence effect do not exist.

Case II The worst case of picket fencing occurs when there is non-periodic extension of **data**

At

$$\omega_0 = \frac{2\pi}{N}k_0 + \frac{\pi}{N}$$

In this case we have

$$\begin{aligned}\cos[\omega_0 (n + N)] &= \cos\left[\left(\frac{2\pi k_0}{N} + \frac{\pi}{N}\right)(n + N)\right] \\ &= \cos\left[\frac{2\pi k_0 n}{N} + 2\pi k_0 + \pi\right] \\ &= -\cos\left[\frac{2\pi k_0 n}{N}\right]\end{aligned}$$

Clearly, we see that the non-periodic extension of data results in a distorted sinusoid. The actual spectral peak does not appear at any of the discrete points. In fact it lies between two consecutive discrete points. The magnitude obtained at the discrete points is not the actual magnitude of the signal at that particular frequency. This case represents the worst case of

the picket fence effect. This effect was encountered during the actual **experimentation**. It can be easily made out because when picket fence effect is not negligible the peaks of harmonic frequencies do not occur at exact multiples of the fundamental. **But** if the **data** length is truncated appropriately then the picket fence effect disappears.

The two main problems associated with the picket fence effect are

- o We cannot identify the correct amplitude and location of the spectral peaks.
- o The strength of side lobes also depends on the location relative to **the** picket.

Care should be taken to prevent this kind of situation in the FFT analysis. In all the experimental cases periodic number of data cycles have been taken to avoid this effect.

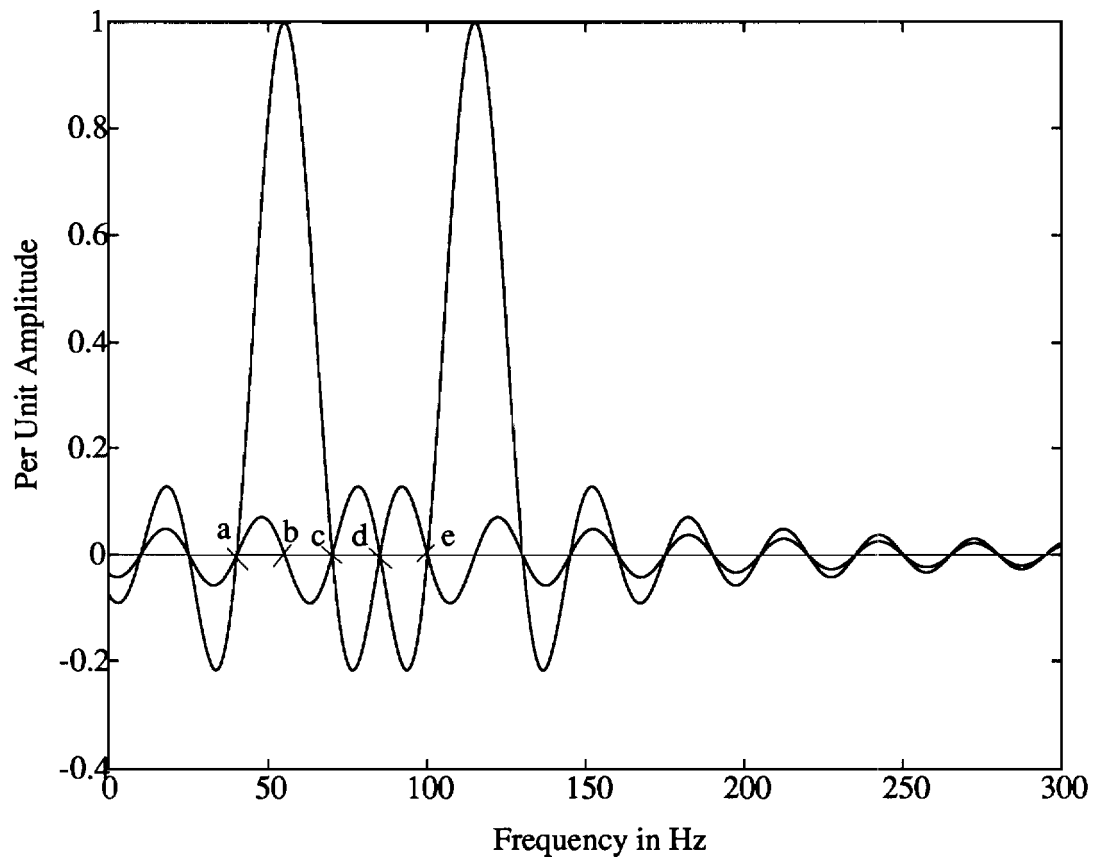


Figure 16. Position of minimum spectral leakage during FFT analysis

CHAPTER 5 AUTOMATION OF **THE** HARMONIC LOAD DETECTION PROCESS USING NEURAL NETWORKS

5.1. Need for Neural Net approach

The problem of harmonic load identification consists of detecting the average power flows at the harmonic frequencies. The processing of the acquired data has been done manually using standard signal processing packages like **Matlab**. This **procedure** can be automated to reduce the amount of time spent on it, and to make it easier **for** other users not familiar with the process. In the present case a Neural Network has been used to do this job, for reasons discussed further in the text. An essential step of the process is the detection of peaks in the FFT analysis on the voltage or current **waveforms**. This step is made more difficult when the fundamental frequency is not known **precisely** and by the fact that the FFT analyses produces a lot of spurious peaks along with the **actual** peaks which indicate the presence of the signal. The spurious peaks can show up in the signal analysis because of reasons like the presence of high frequency noise or any transients in the supply voltage.

Since the controllable parameters in this data acquisition **process are** the sampling rate and the number of data points acquired, we need a versatile and intelligent system which will be able to detect peaks at all the harmonic frequencies under **varying** system conditions. A simple C program might not be able to properly handle the condition of imprecise knowledge of the fundamental , or separate the actual peaks from spurious peaks. Hence there is a need for an intelligent automated system. A **neural** network can be

used to do this job. The net can be trained to recognize the actual peaks at the harmonic frequencies only.

5.2. Introduction to the Neural Network Application

A lot of research is being done on the system identification **problem** using neural networks. A neural network is basically composed of interconnected neurons. Neural networks offer the advantage of performance improvement through **learning** using parallel and distributed processing. These networks are implemented using massive connections among processing units with variable strengths, and hence they are attractive for applications in system identification.

The nature of data received from the FFT analysis of the voltage or current signals is hard to formulate in mathematical terms as there is no fixed relationship between the input data given to the neural net for FFT analysis and the signals present in that particular waveform. Only after the data has been analyzed using FFT techniques that we can detect the presence of any of the frequencies. Thus the mathematical **formulation** of this problem is a difficult task. This problem of harmonic peak identification consists of setting up a suitably parameterized identification model and adjusting the parameters of the model to optimize a performance function based on the error between the input and the identification model outputs. A neural network can perform this function mapping after it has been trained. A single neuron which forms a weighted sum of N inputs and passes the result through a nonlinearity is shown in Figure 17. The output of this neuron is given by

$$y = f \left(\sum_{i=1}^{n-1} w_i x_i \right)$$

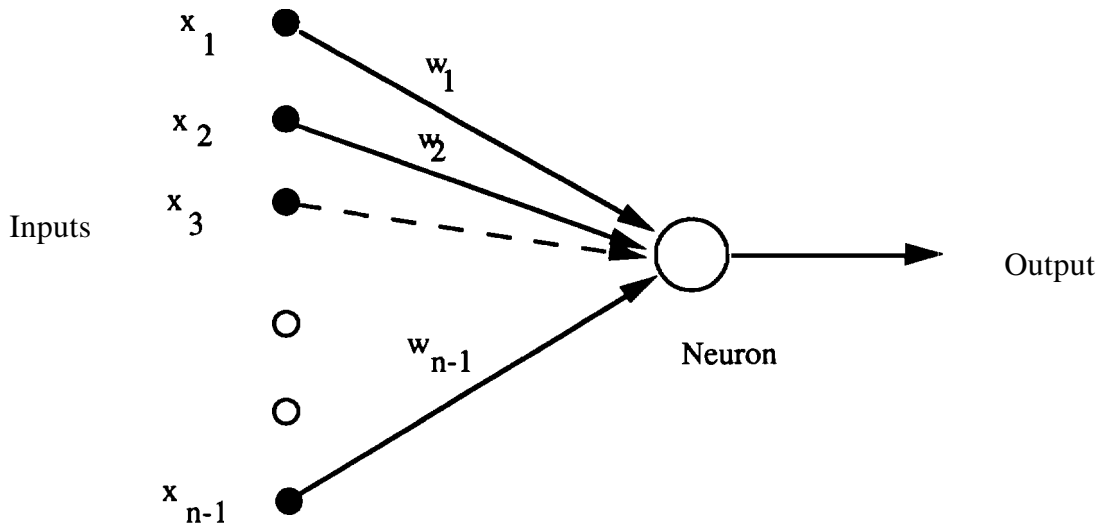


Figure 17. A single neuron which takes N inputs and forms a weighted output

Algorithms which produce an estimation of the system behavior **based** on the observation of input-output measurement pairs fall under the category of system identification techniques. These techniques can be divided into two major groups: parameter estimation, which assumes a known system function with only unknown parameters, and functional estimation which deals with the estimation of the system function as well as its parameters. The popular back-propagation algorithm is used as a functional estimation algorithm in the present work to detect peaks.

5.3. Back Propagation Algorithm

The back-propagation training algorithm is an iterative **gradient** algorithm designed to minimize the mean square error between the actual output of a multilayer feed-forward **perceptron** and the desired outputs. One drawback of the back-propagation algorithm is its requirement of continuous differential nonlinearities. Also, its learning speed is slow. The standard back propagation algorithm as given by Richard P. Lippmann [12] is given below.

The following assumes a **sigmoidal** nonlinearity $f(\lambda)$ where $f(\lambda)$ is

$$f(\lambda) = 1 / (1 + \exp(-\lambda))$$

Step 1. Initialize all weights and node offsets to small random values.

Step 2. Present input and desired outputs. The input could be new on each trial or samples from a training set could be presented cyclically until weights stabilize.

Step 3. Calculate actual outputs using the activation and output functions of each neuron .

Step 4. Adapt weights. Use a recursive algorithm starting at the output nodes and working back to the first hidden layer. Adjust weights by

$$w_{ij}(t+1) = w_{ij}(t) + \eta * \delta_j * x_i'$$

In this equation $w_{ij}(t)$ is the weight from the hidden node i or from an **input** node j at any time t , x_i' is either the output of node i or is an input. η is a gain term and δ_j is an error term for node j . If node j is an output node then

$$\delta_j = y_j (1 - y_j) (d_j - y_j) \quad \dots (5.3)$$

$(d_j - y_j)$ is the error term such that d_j is the desired output at node j and y_j is the actual output.

If the node j is an internal hidden node, then

$$\delta_j = x_j'(1 - x_j') \sum_k (\delta_k w_{jk}) \quad \dots (5.4)$$

where k is all over nodes in the layer above node j .

Convergence can be faster if a momentum term is added and weight changes are smoothed by

$$w_{ij}(t+1) = w_{ij}(t) + \eta \delta_j x_i' + a (w_{ij}(t) - w_{ij}(t-1)) \quad \dots (5.5)$$

where $0 < a < 1$, is the momentum constant

Step 5. Repeat by going to Step 2, until the minimum error criterion has been met.

5.4. Use of the Neural Net on the Computer Monitor data

A neural network program was written in **Matlab**. The structure of the net that was experimented on has 7 input nodes, one hidden layer of 5 nodes, and one output node as shown in Figure 18 below.

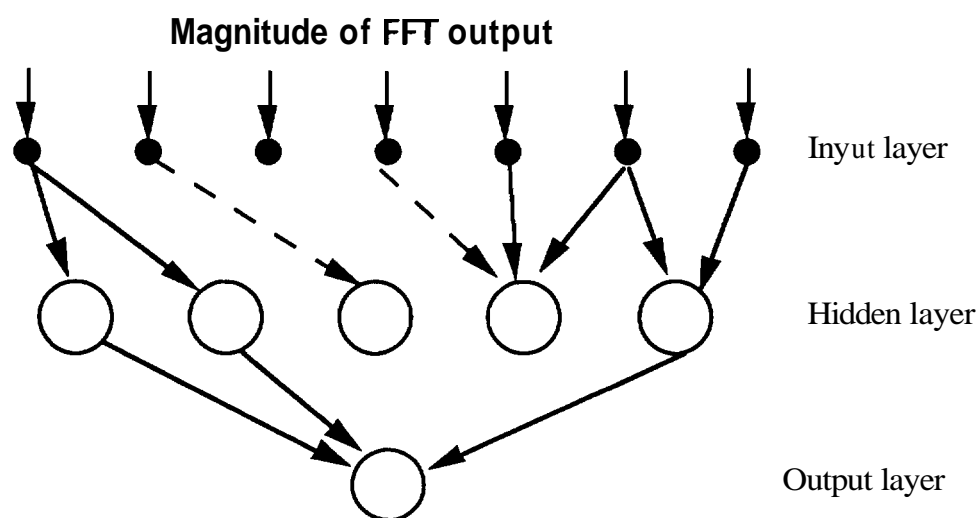


Figure 18 Structure of the Net Used to Identify Harmonic Peaks in FFT Data

5.4.1. Structure of the Neural Net Algorithm

For training purpose the FFT data vector for the voltage waveform taken from the fluorescent lamp experiment was given to the net along with the desired output. A sample of the input and desired output given to the net for training is shown in the Table 3. The desired output has been chosen such that each and every harmonic peak in the FFT data has been assigned a value of **0.9** and every spurious non-harmonic peak a value of **0.1**. In this way, the net is fed data so that it is supposed to detect only the valid harmonic peaks, while

it neglects all the spurious peaks. The point to be noticed is that at least **three** or four peaks are given in the training data so that the net is able to learn the relationship between different harmonic peaks as well.

The net has to be trained with representative data supposedly **similar** to that the net will be used on. For example, with the net trained on FIT data computed from the acquired voltage waveform in the fluorescent lamp case, the net **successfully** identified the harmonic peaks in FIT data taken from the other harmonic loads, such **as** those from the computer monitor, **triac** controlled light dimmers, and the PWM induction motor drive. It is important that the net be trained on data that has **as** much of the features that it would be tested on - in this case waveforms that contains many harmonics. The **neural** net is given a sigmoidal constant ' λ ' of **0.7**, as defined in equation (5.1). The learning constant η is **0.95** and the momentum constant α is **0.95**. The values have been chosen heuristically. Experiments with a lower learning constant η were not successful, hence it has to be changed to the value of **0.95**. The initial values of the weights between the input nodes and hidden layer and the hidden layer and the output nodes has been **initialized** to random values between **+ 0.1**.

The neural net has been trained on **357** points of the input FIT data. To train the net the inputs points **are** given in a staggered set of seven points during each iteration. Using the initial value of the weights the output response at the hidden **and** output layers **are** calculated for all the **357** points in steps of **7** points at a time. After the full set of **357** points have been run through the net, the error values between the actual output and desired output as encountered over this period are calculated, and compared with the maximum allowable error of **0.002**. The hidden weights and the output weights are adjusted in such a way that error value in the next iteration will tend to be lower than the **error** value in the previous iteration. This process of lowering error values is achieved by using the gradient search algorithm. It is repeated till the condition of the allowable error of **0.002** is

encountered. At the end of this training **process** the final value of the weights are set. This set of weights can be used for testing the net on any other set of FFT data.

5.4.2. Testing of the Load Data Using the trained Neural Net

For testing purposes it is convenient to be able to combine the two processes of FFT computation and peak detection by the trained net. A **Matlab** program has been developed for such purposes. It accepts as input the time array of digitized **waveform**, and **performs** an FFT on it. The spectrum magnitude from the FFT output is then **scanned**, seven points at a time, by the trained net. The waveform fed to the net should have an integral number of cycles so that the FFT analysis carried on it is accurate. The net has **been** trained to ignore all the spurious peaks. The neural net gives as output a column vector which indicates the harmonic peaks. Tests were performed on the acquired voltage and current of the loads that we had experimental data on. In each case, the net was able to identify the correct harmonic peaks accurately.

The magnitude and phase angle of the current harmonics at the **same** points, as found on the voltage FFT vector, have been found. Thus the magnitude **and** phase values at these harmonic index points from the voltage and current FFT vectors are taken, and the average harmonic power flowing at that particular harmonic computed from this information. The direction of these average power values determines if the load under test is a harmonic load or not.

For example Figure 19 shows the plot of the voltage harmonic peaks of the computer monitor as indicated by the neural net output with respect to the frequency. The average harmonic powers flowing to the load at different harmonics, as **determined** by the neural network is shown in Table 4.

Table 3 A sample of the Input FFT Data and the Desired Output as given to Neural Net for Training

FFT input	Desired Output
5.5668123e+02	1.0000000e-01
6.1904635e+02	1.0000000e-01
6.6106233e+02	1.0000000e-01
8.4343438e+02	1.0000000e-01
9.6502893e+02	1.0000000e-01
9.1732842e+03	1.0000000e-01
2.0510155e+06	9.0000000e-01
6.6306639e+02	1.0000000e-01
5.1011178e+02	1.0000000e-01
5.3117821e+02	1.0000000e-01
4.5914624e+02	1.0000000e-01
4.4556359e+02	1.0000000e-01
4.7346819e+02	1.0000000e-01
3.0751655e+03	9.0000000e-01
1.7798461e+02	1.0000000e-01
3.1017938e+02	1.0000000e-01
2.5639177e+02	1.0000000e-01
3.3603130e+02	1.0000000e-01
4.3104442e+02	1.0000000e-01
3.9119463e+02	1.0000000e-01
3.0254823e+04	9.0000000e-01
3.6655398e+02	1.0000000e-01
2.1988104e+02	1.0000000e-01
2.3548936e+02	1.0000000e-01
.	.
.	.
2.2998407e+02	1.0000000e-01
.	.
.	.

Table 4 Average Harmonic Powers for Computer Monitor given by Neural Net

Frequency	Average Power in 'watts'
60 Hz.	60.67046
120 Hz.	4.48e-05
180 Hz.	-0.21688
240 Hz.	3.008e-05
300 Hz.	-1.009788
360 Hz.	1.3e-05
420 Hz.	-0.06882
480 Hz.	-2.0636e-05
540 Hz.	-0.023684
600 Hz.	None
660 Hz.	-0.016127
720 Hz.	- 1.6048e-05
780 Hz.	-0.00059004
840 Hz.	3.208e-05
900 Hz.	2.5438e-03
960 Hz.	- 1.2972e-06
1020 Hz.	1.92344e-03
1080 Hz.	- 1.56308e-05
1140 Hz.	8.8628e-04
1200 Hz.	3.9092e-05
1260 Hz.	-2.0596e-03

Table 4, Continued

1320 Hz •	1.51876e-06
1380 Hz.	9.32656e-05
1440 Hz	- 2.45108e-05
1500 Hz	- 8.8416e-05

Comparing the average harmonic power flows as given by the neural net with those in Table 1, we see a small difference in the two corresponding values at some frequencies. This is due to the fact that the error angle, as defined by the difference in phase angle characteristics between the voltage and current amplifiers, has not been taken into consideration in the neural net computation. Since **error** angle is small neglecting it does not cause any difference in the interpretation of the results, when the reverse flow in average power are significant. However in the borderline cases, compensation for the phase angle characteristic can be applied to the time series **data** before applying it to the net.

From the above discussion we see that the neural net can be **trained** and employed to automate the process of determining whether the **data** fed to it is from a harmonic load or not.

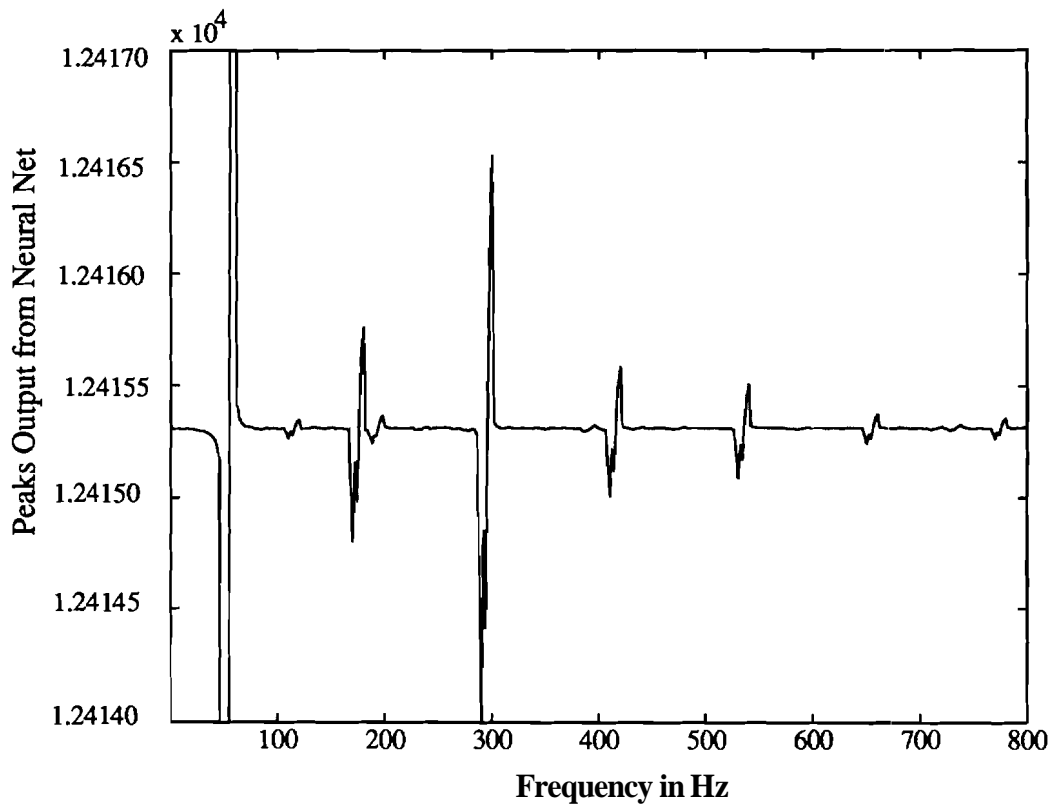


Figure 18 Voltage Harmonic Peaks detected by Neural Net

CHAPTER 6. RECOMMENDED APPLICATION OF THE **DETECTION** TECHNIQUE

6.1. Conclusion

We started with the objective of being able to detect with accuracy the presence of any harmonic injecting loads on the power system. The basis of how **harmonic** current injection takes place in a harmonic load has been explained in this present work. As has been proven, such a condition can be detected by measuring the average power flows at harmonic frequencies for the load under test. The experimental results have supported the theoretical analysis.

There are certain precautions which should be taken during and **after** experimentation, before making a final conclusion on the nature of the **load** under test. For correct interpretation of the FFT results it is important that the signal be in its steady state. There can be a small drift in the fundamental frequency during data acquisition, which will show up as noise in the signal. Large drifts can give erroneous results. Also, in some cases the harmonic signal in the FFT plot has a small value and as such it cannot be easily distinguished from the noise around it, the results of the FFT analysis for that particular harmonic will not be reliable. Results of such low magnitude harmonic signals should not be the basis for declaring the load under test as a harmonic load. Errors because of spectral leakage can be reduced using standard windowing techniques to the signal data acquired.

Using all the precautions mentioned in this work, the results of **the** FFT analysis on the voltage and current data acquired will easily determine whether the load is a harmonic load with the use of the proposed method.

6.2. Detection technique configuration

As has been defined in the standards that the total harmonic distortion (THD) should not exceed the specified limit. In all practical cases the interface between the customer mains and the utility supply conductors referred to as the 'point of common coupling' is used as the point of focus for all measurements as far as power quality is concerned. If there is a net transfer of energy from the customer back to **the** utility, at any harmonic frequency then as shown above, it proves the presence of a nonlinear load on the customer's side. By taking a look at the power flow measurements at the mains we can simply make out the presence of the nonlinear load. However to locate the load which is responsible for the harmonics on the customer side, we need to use this measurement and analysis technique iteratively. It means that we need to go down from the mains level to the actual outlet level iteratively to pin-point the actual harmonic load. Once the search has been narrowed down to a few loads, then the measurement and average power analysis can be **carried** out again to find out the magnitudes of individual harmonic **current** levels flowing in the circuit. At this point we can use any of the known filtering techniques to filter out the troublesome harmonic as per IEEE 519 or other harmonic standards.

The point to be noted here is that the absence of harmonic at the mains level does not necessarily mean the absence of harmonic loads on the particular customer site. If there are a number of harmonic loads at the customer site, in that case it is probable that the analysis at mains will not reveal the presence of the harmonic loads down the line from the point of common coupling. This is on account of fact each nonlinearity is unique. The total current, at a particular harmonic, at the mains is a vector sum of the individual harmonic current coming out from each and every harmonic load. There is a possibility that a certain combination of harmonic loads may interact with each other that each one of them is acting as a compensator of the phase angle for the rest such that the phase angle between current and voltage for a particular harmonic at the point of **common** coupling falls

between the allowable limits of 90°. This kind of situation will hide the true nature of the electrical loads connected on the customer site. But at the same time we know that a lot of harmonic loads do not have a fixed non-linearity (Loads like fluorescent lamps, adjustable speed drives etc.). Dynamically changing nonlinearity implies that such a deceiving situation may show up at a certain time but will not be seen at a certain other time. To circumvent this problem it would be necessary to take a number of measurements at different times to eliminate this low probability occurrence.

6.3. Suggestions for Future Research

The importance of power quality is increasing day by day. A lot of complex issues relating to harmonic flows in the power system have to be resolved in order to maintain the power quality as has been defined by various harmonic standards. Detection of harmonic loads on the power system is one step towards that direction. Correct filtering methods have to be employed at various nodes in the power system to filter out the troublesome harmonics. Issues relating to harmonic resonance have to be addressed properly in order to avoid unnecessary damage to the various electrical components in the system.

The overall effect of the source and circuit impedance in the power system on power quality, under the presence of harmonics has to be understood fully. In order to do understand the phenomenon of generation of harmonics better much more effort is needed towards the modeling of harmonic loads in general. Some research in this direction has already been published by Donald Weiner and John Spina [3]. But there is still a need for a comprehensive model of nonlinearity in general.

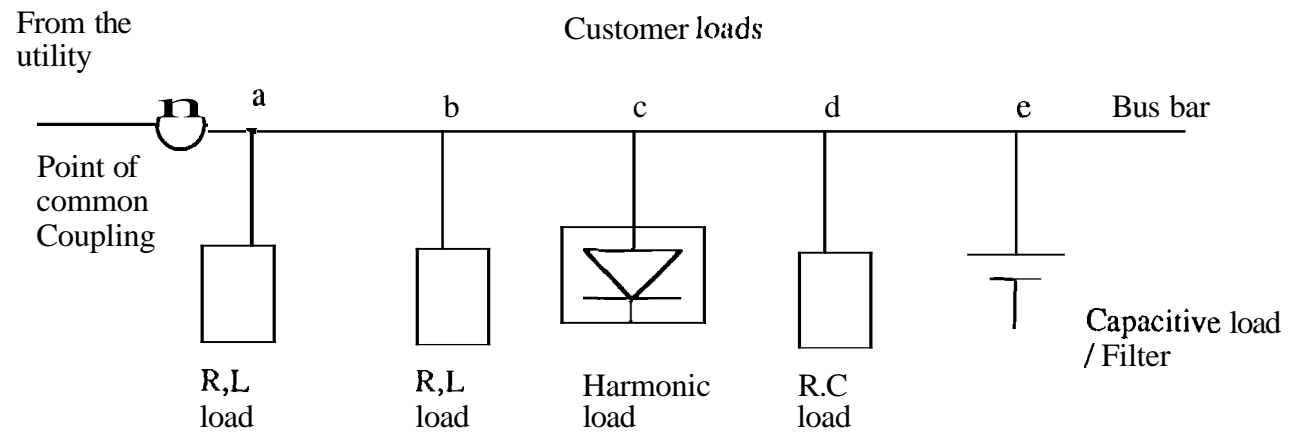


Figure 20. Measurement taken iteratively at different customer points

BIBLIOGRAPHY

- [1] W. Shepherd, P. Zand, "Energy Flow and Power Factor in **Non-Sinusoidal Circuits**", Cambridge University Press, 1979.
- [2] Alan V. **Oppenheim** and Ronald W. Schafer, "Digital Signal Processing" **Prentice Hall Inc**, 1975.
- [3] Donald D. Weiner and John F. Spina, "Sinusoidal Analysis and Modelling of Weakly Nonlinear Circuits", **Van Nostrand Reinhold Company**, 1980.
- [4] K. G. Beauchamp, "Signal Processing", George Allen & Unwin Ltd. London, 1973.
- [5] M. F. **McGranaghan**, J. H. Shaw, R. E. Owen, "Measuring Voltage and Current Harmonics on Distribution Systems" **IEEE Transactions on Power Apparatus and Systems**, Vol. **PAS-100**, No. 7, July 1981.
- [6] Timothy A. George and David Bones, "Harmonic Power Flow Determination using the Fast Fourier **Transform**" **IEEE Transactions on Power Delivery** Vol. 6, No. 2, April 1991.
- [7] James K. Phipps, John P. Nelson, Pankaj K. Sen, "Power Quality & Harmonic Distortion on Distribution Systems" **IEEE Rural Electric Power Conference**, 35th Annual Meeting 1991.
- [8] D. G. Flinn, C. Gilker, S. R. **Mendis**, "Methods for Identifying Potential Power Quality Problems" **IEEE Rural Electric Power Conference**, 35th Annual Meeting 1991.
- [9] R. R. Verderber, O. C. Morse and W. R. Alling, "Harmonics from Compact Fluorescent Lamps", **IEEE Industry Application Society Annual Meeting** 1991.
- [10] John K. Winn, **Daryld** Ray Crow, "Harmonic Measurement Using a Digital Storage Oscilloscope", **IEEE Transactions on Industry Applications**, Vol. 25, **No.4, July/August** 1989.
- [11] Joseph S. **Subjak** and John S. **McQuilkin**, "Harmonics - Causes, Effects, Measurements, and Analysis: An Update", **IEEE Transactions on Industry Applications**, Vol. 26, **No.6, Nov/Dec**. 1990.
- [12] Richard Lippman, "An Introduction to Computing with **Neural Nets**", **IEEE Acoustic Speech and Signal Processing Magazine**, April 1987, pp. 4 -22.

- [13] Guy Lemieux, "Power System Harmonic Resonance - A Documented Case", IEEE Transactions on Industry Applications, Vol. 26, No. 3, May/June 1990.
- [14] Alay A. Mahmoud and Richard D. Shultz, "A method for Analyzing Harmonic Distribution in A.C. Power Systems, IEEE Transactions on Power Apparatus and Systems, Volume PAS-101, No. 6, June 1982.
- [15] J.F. Eggleston, J. Arrillaga and A. Semlyen, "Analysis of the Harmonic Distortion resulting from the interaction between Synchronous Machines and HVDC convertors", Vol. 3, No. 1, January 1988.
- [16] "IEEE Recommended Practices and Requirements for Harmonic Control in Electrical Power Systems", IEEE Standard 519-1992.